1 **Living, dead, and absent trees - How do moth outbreaks shape small-scale patterns of soil**

2 **organic matter stocks and dynamics at the Subarctic mountain birch treeline?**

3

4 **Running Title:** Effect of moth outbreaks on soil C stocks

5 Nele Meyer[1,2], Yi Xu[1], Katri Karjalainen[3], Sylwia Adamczyk[1,4], Christina Biasi[3], Lona van Delden[3,5], Angela

6 Martin[1], Kevin Mganga[1,6], Kristiina Myller[3], Outi-Maaria Sietiö[1], Otso Suominen[7], Kristiina Karhu[1,8]

7

8 [1]Department of Forest Sciences, Faculty of Agriculture and Forestry, University of Helsinki, P.O. Box 27, 00014 Helsinki,

9 Finland

10 [2]Department of Soil Ecology, University of Bayreuth, Dr.-Hans-Frisch-Straße 1-3, 95448 Bayreuth, Germany

11 [3]Department of Environmental and Biological Sciences, University of Eastern Finland, Yliopistonranta 1, 70210,

12 Kuopio, Finland

13 [4]Natural Resources Institute Finland (Luke), Latokartanonkaari 9, 00790 Helsinki, Finland

14 [5]Alfred Wegener Institute Helmholtz Centre for Polar and Marine Research, Telegraphenberg A45, 14473 Potsdam,

15 Germany

16 [6]Department of Agricultural Sciences, South Eastern Kenya University, P.O. Box 170-90200, Kitui, Kenya

17 [7]Biodiversity Unit, Kevo Subarctic Research Institute, University of Turku, 20014, Turku, Finland

18 [8]Helsinki Institute of Life Science (Hilife), University of Helsinki, Finland

19

20 **Corresponding author:** Nele Meyer (nele.meyer@uni-bayreuth.de, +49(0)921555610)

21

22 **Keywords**

23 Soil organic carbon, soil respiration, priming effect, microbial N mining, deadwood

24

25 **Abstract**

26 Mountain birch forests (*B. pubescens* Ehrh. ssp. *czerepanovii*) at the subarctic treeline not only benefit from

27 global warming, but are also increasingly affected by caterpillar outbreaks from foliage-feeding geometrid

28 moths. Both of these factors have unknown consequences on soil organic carbon (SOC) stocks and

29 biogeochemical cycles. We measured SOC stocks down to the bedrock under living trees, as well as under two

30 stages of dead trees (12 and 55 years since moth outbreak) and treeless tundra in northern Finland. Further, we

31 measured in-situ soil respiration, potential SOC decomposability, biological (enzyme activities, microbial

32 biomass), and chemical (N, mineral N, pH) soil properties. SOC stocks were significantly higher under living

33 trees (4.1±2.1 kg m²) than in the treeless tundra (2.4±0.6 kg m²), and remained at an elevated level even 12

34 (3.7±1.7 kg m²) and 55 years (4.9±3.0 kg m²) after tree death. The effect of tree status on SOC stocks decreased

35 with increasing distance from the tree and with increasing depth, i.e. a significant effect of tree status was

36 found in the organic layer, but not in mineral soil. Soil under living trees was characterized by higher mineral

37 N contents, microbial biomass, microbial activity, and soil respiration compared with the treeless tundra; soils

38 under dead trees were intermediate between these two. The results suggest accelerated organic matter turnover

39 under living trees but a positive net effect on SOC stocks. Slowed organic matter turnover and continuous

40 supply of deadwood may explain why SOC stocks remained elevated under dead trees, despite the heavy

41 decrease in aboveground C stocks. We conclude that the increased occurrence of moth damage with climate

42 change would have minor effects on SOC stocks, but ultimately decrease ecosystem C stocks (49% within 55

43 years in this area), if the mountain birch forests will not be able to recover from the outbreaks.

44

45 1. **Introduction**

46 Mountain birch (*B. pubescens* Ehrh. ssp. *czerepanovii*) is the dominant tree species at the subarctic treeline of

47 Fennoscandia, and significantly contributes to the CO_2 sink capacity of subarctic landscapes (Christensen et

48 al., 2007). Due to climate warming and increased nitrogen (N) deposition, an advance of the treeline has been

49 observed in recent decades (Hofgaard et al., 2012; Rundqvist et al., 2011; Tømmervik et al., 2004). Global

50 warming has also led to a drastic increase in insect herbivory over the past decades (Hagen et al., 2007; Jepsen

51 et al., 2007; Neuvonen et al., 1999). Insect herbivory has been shown to have immense impacts on plant growth

52 and carbon (C) fluxes, even at background intensities (Silfver et al., 2020), but outbreak intensities in particular

53 cause large natural disturbances. For instance, Heliasz et al. (2011) reported an 89% reduction of the C sink

54 strength upon defoliation of mountain birch by larvae of autumn and winter moths. In Fennoscandia, outbreaks

55 of caterpillars from foliage-feeding geometrid moths (*Epirrita autumnata* and *Operophtera brumata*) occur at

56 intervals of around 10 years. While mountain birch can compensate defoliation to some extent (Huttunen et

57 al., 2012), intense damage in such nutrient-poor soils and in cold climatic conditions often leads to forest

58 dieback, leaving large areas of deadwood behind (Tenow, 1996). Considering that 5,000 km^2 of mountain birch

59 forest were affected in the 1960's in northern Finland alone (Nuorteva, 1963), and 10,600 km^2 during the

60 2000's in northern Fennoscandia (Jepsen et al., 2009), this issue is of quantitative relevance. High intensity

61 summer grazing by reindeer compounds the issue by impeding the growth of new birch seedlings and basal

62 sprouts, especially in Finnish Lapland (Lehtonen & Heikkinen, 1995; Kumpula et al., 2011; Biuw et al., 2014).

63 The combination of grazing and moth damage induces a conversion of former forests into treeless tundra

64 vegetation, resulting in immense reductions of tree primary production (Olsson et al., 2017), and thus, CO_2

65 sequestration potential.

66 The consequences of treeline advance or forest dieback on aboveground C storage are straightforward and

67 frequently studied (Dahl et al., 2017; Rusell et al., 2015), however, the consequences on soil organic carbon

68 (SOC) stocks are rather uncertain. Several studies have shown that an advance of the treeline may deplete SOC

69 stocks (Clemmensen et al., 2021; Friggens et al., 2020b; Hartley et al., 2012; Wilmking et al., 2006) despite C

70 input via litter and roots. For instance, Parker et al. (2015) showed that SOC stocks of organic layers were

71 considerably lower in forested plots (2.04±0.25 kg m^2) than at heath plots (7.03± 0.79 kg m^2). This may be

72 explained by a phenomenon termed the "priming effect" (Fontaine et al., 2004; Kuzyakov, 2000): a labile C

73 supply from root exudates or fresh litter can stimulate microbial decomposition of older soil organic matter

74 (SOM). In this context, it is assumed that microbes increasingly decompose SOM in order to acquire N from

75 it ("microbial N-mining"; Craine et al., 2007; Moorhead & Sinsabaugh, 2006), which is particularly relevant

76 in N-poor subarctic soils (Hicks et al., 2020).

77 Reversing this finding, it may be speculated that despite the decrease in tree primary production, forest dieback

78 caused by moth outbreaks can induce an increase of SOC stocks, for at least five reasons. First, root exudation

79 decreases, which then causes a decrease in labile C that can stimulate priming. Second, insect herbivory

80 induces an abrupt return of available N and other nutrients to soils via frass (Kaukonen et al., 2013; Parker et

81 al., 2017). Together with the lower N demand of dead trees, the limits on N may be released, hence N-mining

82 and associated priming become unnecessary in soil that is no longer N-limited. Third, large amounts of organic

83 matter are returned to the soil via decomposing roots and deadwood (Kosunen et al., 2020). Since SOM

84 decomposes slowly in cold climates, and parts of SOM are recalcitrant or stabilized and can remain in soil for

85 hundreds or thousands of years (Lehmann & Kleber, 2015; Schmidt et al., 2011), elevated SOC stocks may

86 persist in the long-term. Fourth, temporal patterns of deadwood decay usually follow a negative exponential

87 curve (Mackensen and Bauhus, 2003), i.e. SOM turnover rates may slow down once the most labile compounds

88 of decaying wood have been mineralized. Fifth, insect herbivory has been found to change vegetation

89 composition from shrub-dominated to grass-dominated plant communities (Karlsen et al., 2013), possibly

90 associated with larger organic matter input into soil. Indeed, reduced soil CO_2 efflux has been observed

91 immediately after a defoliation event (Parker et al., 2017) and 8 years thereafter (Sandén et al., 2020),

92 suggesting slowed biochemical cycling. However, despite decreased turnover rates, Sandén et al. (2020) found

93 no difference in SOC stocks 8 years after a defoliation event of subarctic mountain birch in northern

94 Fennoscandia.

95 Interestingly, the opposite effect (i.e. higher resource turnover rates in the short-term) have been observed after

96 moth outbreaks (Kaukonen et al., 2013; Kristensen et al., 2018), mainly linked to increasing concentrations of

97 soil mineral N and labile C from moth frass. According to Kaukonen et al. (2013), moth outbreaks represent a

98 shortcut in C and N input to soils, which bypasses the main routes of carbon from plants to the soil via

99 mycorrhizal and litter-decomposing fungi. However, it remains uncertain whether this effect persists in the

100 long-term. From a study on coniferous forests, Štursová et al. (2014) speculated that the rate of decomposition

101 decreases as soon as the one-time litter input had been processed. Similarly, Kristensen et al. (2018) assumed

102 that such increased turnover rates are mainly short-lived effects, while lower turnover rates can be expected in

103 the long-term. Overall, the temporal effects of moth outbreaks and associated tree death on SOM stocks and

104 biochemical cycling are poorly understood. In particular, the long-term effects are not well quantified.

Former studies on the effect of treeline advance or retreat suffer from the drawback that forested sites are compared with separate tundra sites, or forested sites with defoliated sites, respectively (Hartley et al., 2012; Wilmking et al., 2006). Such space-for-time substitutions are prone to confounding effects, such as differences in temperature, nutrients, or water availability between sites. In this context, it remains unknown whether specific factors (e.g. microclimate) that trigger tree growth, moth outbreaks, or tree survival can also affect SOC turnover rates, i.e. there is no causal link between elevated SOC stocks and trees. This drawback can be overcome by investigating differences between living trees, dead trees, and treeless tundra on a small spatial scale of individual trees, thereby reducing the risk of confounding factors. On a small scale, Friggens et al. (2020a) identified decreasing SOC stocks with distance from the tree, suggesting accumulation of organic matter close to trees, which opposes the conclusions based on comparisons of separate sites.

Here, we conducted a small-scale space-for-time approach on three independent sites by comparing SOC stocks and biochemical properties of soil under four tree statuses: living trees, dead trees (12 years since moth outbreak), dead trees (55 years since moth outbreak) and treeless tundra. These four statuses co-exist at the study sites. We hypothesized that (1) living trees have lower C stocks compared to treeless tundra. Such a negative net effect of a living tree could be caused by the N-demand by the tree stimulating SOM turnover to such an extent that it exceeds the C input from birch trees. Further, we hypothesized (2) that tree death causes the C stocks to develop towards the C stocks of the treeless tundra. This is based on the assumption that SOC decomposition slows down in the absence of trees and root exudates.

2. Materials and methods

2.1 Study area

The study area (69°9'N, 27°9'E, 130-156 m a.s.l.) is located in Northern Finnish Lapland, 12 km south of the village Nuorgam, approximately 5 km west of Lake Pulmankijärvi (Fig. 1). The mean annual temperature was -1.6°C and mean annual precipitation was 448 mm during the time period 1981-2010, measured in Utsjoki, 35

km west of the study site (Finnish Meteorological Institute, 2020). Soils in this region are Podzols on sandy texture (WRB, 2015) and are not affected by permafrost.

The area is a heavily grazed year-round pasture area of the Kaldoaivi reindeer herding cooperative. The herding of such semi-domesticated reindeer by the Sámi people has been practiced since centuries in this area (Kortesalmi, 2008). Reindeer densities in the Kaldoaivi area are around 2.38 reindeer/km² (2006-2007, Biuw et al., 2014). This density remained on average at a same level since the 1950's with the exception of two short-term drops in the late 1960s and mid 1970s and a short-term peak during the 1980s with 4.5 reindeer/km² (Biuw et al., 2014; statistics from the Reindeer Herders Association for reindeer numbers during 1960-2020). The trends in reindeer population densities are quite similar in the neighboring areas in Finland and in Norway, although the overall densities in Norway are slightly lower (i.e. 1.56 reindeer/km² in 2006-2007; Biuw et al., 2014). Traditionally, reindeer migrated between summer pastures in the coastal areas of the Arctic Ocean in Norway and winter pastures in the interior areas of Finland and Norway (Oksanen & Virtanen, 1995). Seasonal migration is still practiced in the neighboured areas in Norway. The contrasting year-round grazing in northernmost Finland results from the fact that seasonal reindeer migration is prevented by law since 1852 (Stark et al., 2021 Kortesalmi, 2008). Although rotational grazing on designated summer and winter pastures has been realized by means of fences in several Finnish districts, no such measures apply to the Kaldoaivi district (Biuw et al., 2014).

During the last century, the study area has been affected by two severe moth outbreak periods. The first occurred between 1960 and 1965, i.e. approximately 55 years before sampling ("$dead_{55}$"); the second was between 2006 and 2008, i.e. approximately 12 years before sampling ("$dead_{12}$"), as previously described (Kaukonen et al., 2013; Lehtonen & Heikkinen, 1995; Saravesi et al., 2015). Since some trees survived the respective outbreaks, the area is characterized by a mosaic that includes living trees (Fig. 2a), dead but still standing trees ($dead_{12}$, Fig. 2b), largely decomposed dead trees with only a stump remaining ($dead_{55}$, Fig. 2c), and treeless tundra vegetation (Fig. 2d).

We conducted a small-scale space-for-time substitution approach to investigate the effect of living trees, dead trees, and treeless tundra on SOC stocks and dynamics. Three independent sites were selected, each approximately 1 ha in size and located approximately 2 km away from each other. Criteria for selecting sites

157 were that 1) all tree statuses (i.e. living, dead$_{12}$, and dead$_{55}$, treeless tundra) were present, each with several

158 randomly distributed individuals, 2) the altitude of the sites was similar, and 3) the sites were located on a flat

159 area to minimize differences in climate and microclimate between and within the sites. At each site, we selected

160 four plots of each of the four tree statuses. Each plot had a size of 3.14 m², i.e. 1 m radius around the tree or

161 plot center, in the case of treeless tundra. Plots were chosen such that the next living or dead tree was at least

162 2 meters away.

163

164 2.2 Understorey vegetation

165 The percentage of understorey vegetation cover was assessed at the species level by visual estimation within

166 a circle of 1 m radius (Fenner, 1997). A few species were unidentifiable; these were grouped into the category

167 of either "other grass species" or "other lichen species".

168

169 2.3 Soil temperature and moisture

170 Between the beginning of July and end of September 2019, we measured soil temperature and volumetric

171 water content (VWC) four times, parallel to the measurements of soil + understorey respiration (see section

172 2.7). Soil temperature and VWC were measured at a depth of 5 cm. The VWC was measured at 5 locations

173 around the respiration collar using a TDR sensor.

174 At each site, 2 plots per tree status were selected for temperature logging. Temperature loggers (Maxim iButton

175 miniature temperature loggers, DS1922L) were buried at 10 cm depth and at 50 cm from the tree or plot center,

176 in the case of treeless tundra. Temperature loggers were inserted at the end of July 2019, and remained in the

177 soil for almost 1 year (with 13 days missing in July 2020) in plastic bags to prevent water damage. Temperature

178 was recorded 4 times per day. The monthly mean temperature and the mean annual temperature were calculated

179 for each plot.

180

181 2.4 Aboveground and belowground plant carbon stocks

182   For living and dead$_{12}$ trees, we measured the height of the trunk and the diameter at breast height (DBH, at 1.3

183   m above ground). In case of bifurcation within the first 1.3 m, the DBH and height of each trunk was recorded

184   separately. Using this data, we calculated aboveground biomass according to Starr et al. (1998).

185   For dead$_{55}$ trees, the height and diameter of the remaining stump were measured. Biomass of dead$_{55}$ trees was

186   estimated according to equation 1, where density was assumed to be $\rho = 478$ kg/m^3, as reported for living trees

187   of *Betula pubescens* (Heräjärvi, 2004).

188   Aboveground tree biomass (kg) $= \rho \times \pi \times r^2 \times h$ (equation 1)

189   Since the abovementioned equation applies to living trees, we corrected the biomass for density loss using

190   annual decay rate constants of 4.5% upon tree death, which has been demonstrated for birch trees (Krankina

191   & Harmon 1995). Tree roots were estimated to be 29.2% of total tree biomass as suggested by Smith et al.

192   (2016), i.e. by dividing aboveground biomass by 70.8 and multiplying by 29.2. The proportion of carbon in all

193   plant biomass pools was assumed to be 50% (Köster et al. 2015).

194   Understorey aboveground biomass was calculated by harvesting all understorey vegetation including moss and

195   lichen from the respiration collars (20 cm diameter, see 2.7, Fig. 1f) at the end of the experiment. Plants were

196   dried at 60°C and weighed. Assuming that vegetation inside the collars is representative of the entire plot, we

197   extrapolated understorey biomass to an area of 1 m radius around each tree or plot center. To determine

198   understorey root biomass, we took samples from 3 locations around each tree with an auger of 5 cm diameter

199   (total organic layer + 10 cm of mineral soil, see section 2.5; white circles in Fig. 1f), and combined these to a

200   composite sample per plot. Understorey roots were isolated from the organic layer by sieving to 2 mm and

201   subsequent washing. Such data were extrapolated to an area of 1 m radius around the plot center. C content

202   was assumed to account for 50% of the biomass. The mineral soil contained no visible roots from understorey

203   vegetation.

204

205   2.5 Determination of SOC stocks

206   To determine SOC stocks ("stock sample set", Fig. 1f), 10 auger samples (2.5 cm diameter) were taken from

207   25 cm, 50 cm, 75 cm, and 100 cm distance around the stem, or around the plot center in the case of treeless

208 tundra (black dots in Fig. 1f). The organic layer, the eluviated E horizon, and the illuviated B horizon up to a

209 depth at which the auger could not be inserted any deeper (assuming that bedrock or large rocks were reached,

210 cf. Parker et al., 2015) were taken separately. The thickness of each layer and the maximum depth of mineral

211 soil were recorded for each of the 40 sampling points per plot. The auger samples were combined to form one

212 composite sample from each distance and horizon per plot. Samples were dried at 40° immediately after

213 sampling, subsequently sieved to 4 mm (organic) and 2 mm (mineral), and milled. The C and N contents were

214 measured with VarioMax CN analyser (Germany). Since soils in this area are not calcareous (Hinneri et al.,

215 1975) and our samples had a pH < 6, the measured C contents were assumed to equal SOC.

216 Bulk density of the organic layer was measured at 3 locations 50 cm from each tree or plot center (white circles

217 in Fig. 1e) by drilling a sharp root auger (5 cm diameter) into the organic layer, measuring its thickness and

218 resultant volume, and drying at 105°C. There was no obvious compression of the organic layer using the root

219 auger. Bulk density of the mineral soil was determined by taking 1-2 soil cylinders (170 cm³) 50 cm from each

220 tree or plot center. The volume of rock fragments >2 mm was subtracted from the cylinder volume to calculate

221 bulk density of fine earth. To avoid error propagation, the average bulk density and stone content per site and

222 tree status was used in calculations for organic layer and mineral soil, respectively. We are aware that soils

223 also contain large rocks that were not included in the calculation of rock fragments from the soil cylinders.

224 However, large rocks determined the maximum depth that could be sampled and were therefore included in

225 the calculation of SOC stocks.

226 SOC stocks were calculated by equation 2 and expressed as kg m².

227 Stock (t ha^{-1}) = C content (%) x bulk density of fine earth (g cm³) x thickness (cm) x (1 – rock fragments [%]

228 / 100)   (equation 2)

229 To calculate overall stocks within a 1 m radius around a tree, SOC stocks were calculated for each distance

230 separately, then multiplied with the respective area and summed, i.e. we calculated total stocks within an area

231 of 3.142 m^2. For the treeless tundra, stocks were calculated similarly around the center of the plot. Note that

232 mineral soil was always sampled up to the bedrock. Hence, calculated stocks represent total stocks, but do not

233 refer to a standardized depth. The maximum sampled depth was 70 cm of mineral soil, but such depths were

234 only reached occasionally and not consistently within a given plot or distance around a tree. The average depth

235 of mineral soil across all sites and plots was 6 cm.

236 Stocks of total soil N were calculated analogously to SOC stocks.

237

238 2.6 Soil biological and chemical properties

239 For soil properties other than C and N stocks, we took samples 50 cm from the tree or plot center ("process

240 sample set", small grey dots in Fig. 1f). According to Parker et al. (2017), this is the distance at which the

241 effect of tree status may be the greatest. At least 5 samples were taken from each plot using an auger (5 cm

242 diameter). Additional samples were taken if collected soil material was not sufficient. We sampled the entire

243 organic layer and the mineral soil up to 10 cm depth (i.e. composite of E and B layer). Samples were combined

244 to form one composite sample per plot and soil layer (organic, mineral). Samples were kept in the fridge and

245 sieved to 4 mm (organic) and 2 mm (mineral) within 1 week after sampling. Roots were removed, and samples

246 were then split into separate bags and either dried (40°C), stored cold (8°C), or kept frozen (-20°).

247 Soil C and N contents were also measured as described above from dried soil for the process sample set.

248 Soil pH was measured from 1:2 soil-water slurry with a WTW electrode (Xylem Analytics, Germany).

249 Mineral N in the form of nitrate (NO_3^-) and ammonium (NH_4^+) was determined according to Carter &

250 Gregorich (2008) from frozen soils after allowing the soil the thaw for 2 days. Mineral N was extracted from

251 ~30 ml of soil with 100 ml 1M KCl solution and analyzed by spectrophotometry (PerkinElmer - 1420

252 VICTOR[3]™, United States) according to Miranda et al. (2001). Mineral N content was calculated per g dry

253 weight of soil.

254   For lab-based respiration measurements, frozen soils were thawed at 5°C for 2 days. An amount of soil

255 corresponding to 8 g (organic) or 30 g (mineral soil) of dry weight was filled into incubation vessels, two

256 replicates per sample, and subsequently rewetted to 50% of water holding capacity (WHC) with distilled water,

257 if necessary. Soil was pre-incubated at 20°C for 5 days. Basal respiration was then measured for 8 days,

258 expressed as the average hourly CO_2 production per g soil or per g SOC, respectively. After measurement of

259 basal respiration, glucose was added to each vessel at 8 mg glucose g^{-1} dry soil in aqueous solution (3.5 ml per

260 vessel for organic layer, and 1.5 ml per vessel for mineral soil) – but not exceeding 60% WHC of soil. After

261 the addition of glucose, soil respiration was measured for 100 hours. This so-called substrate induced

262 respiration (SIR) was originally developed to estimate the amount of microbial biomass in soils (Anderson &

263 Domsch, 1978), but has subsequently often been used to assess microbial activities and characteristics

264 (Blagodatsky et al., 2000). Here, we used it to determine microbial biomass carbon and investigate the degree

265 of nutrient deficiency. According to Nordgren (1992) and Meyer et al. (2017, 2018), mineralization of glucose

266 depends on nutrient supply of microbes, hence the potential to mineralize glucose serves as an indicator of

267 nutrient availability to microbes. In mineral soil, we additionally tested whether N is the most limiting nutrient

268 by subsequently adding 1.03 mg of $(NH_4)_2SO_4$ per g of soil (DIN ISO 17155, 2013) in aqueous solution to one

269 of the two incubation vessels per sample. Soil in the second incubation vessels received the same amount of

270 water. If such N addition evokes an increase in CO_2 release, this would suggest that N was the most limiting

271 nutrient and hindered the complete mineralization of glucose. We continued measuring CO_2 evolution for 2

272 days. The CO_2 production was measured using an automated respirometer that allows incubating 95 samples

273 in parallel (Respicond, Nordgren Innovations AB, Sweden). The system provides a continuous measurement

274 of CO_2 evolution by trapping CO_2 in potassium hydroxide (KOH) (Nordgren, 1988). Decrease in electrical

275 conductivity in KOH solution caused by CO_2 entrapment was automatically measured every 60 minutes (basal

276 respiration) or 30 minutes (after glucose addition) by platinum electrodes, and the changes in conductivity

277 were automatically transformed to evolution rates based on equation 3, where A is a conductivity constant that

278 depends on the molarity of the KOH solution, C_{t0} is the conductance of the fresh KOH measured at the

279 beginning of the incubation time, and C_{t1} is the conductance at time t.

280 $CO_2 = A \times (C_{t0} - C_{t1}) / C_{t0}$ (equation 3)

281 We calculated the cumulative CO_2 evolution within 100 h after glucose addition (SIR_{cum}). Microbial biomass

282 carbon (MBC) was derived from the maximum initial respiratory response according to Anderson & Domsch

283 (1978) as follows:

284 MBC ($\mu g\ g^{-1}$ soil) = ($\mu l\ CO_2\ g^{-1}$ soil h^{-1}) x 40.04 + 0.37   (equation 4)

285 Enzyme activities were determined from thawed frozen soil. We measured the activities of cellobiosidase (EC

286 3.2.1.91), β-glucosidase (EC 3.2.1.21), chitinase (EC 3.2.1.14), leucine amino-peptidase (EC 3.4.11.1), acid

287 phosphatase (EC 3.1.3.2), β-xylosidase (EC 3.2.1.37), and N-acetyl-glucosaminidase using fluorometric

288 substrates as described in Bell et al. (2013). Briefly, soil suspensions were obtained by mixing 2 g soil with

289 100 ml of 100 mM sodium acetate buffer (pH 5.5) in a mortar for 1 min. These soil suspensions were

290 continuously stirred on a magnetic stirrer. A reaction mixture was prepared by mixing 200 µl of soil suspension

291 with 50 µl of substrate in microplates (96-well); for the blank, 200 µl of buffer and 50 µl of the respective

292 substrate were used. All substrates were ordered from Sigma-Aldrich: 4-methylumbelliferyl β-D-cellobioside

293 (substrate for cellobiosidase), 4-methylumbelliferyl D-glucopyranoside (β-glucosidase), 4-

294 methylumbelliferyl-N-acetyl-β-D-glucosaminide (chitinase), leucine-aminomethylcoumarin (leucine amino-

295 peptidase), 4-methylumbelliferyl phosphate acid (acid phosphatase), 4-methylumbelliferyl-β-D-xyloside (β-

296 xylosidase). The plates were incubated for 140 min at room temperature (20°C) and enzymatic reactions were

297 stopped by adding 10 µm 1M NaOH, except for leucine-aminopeptidase. Fluorescence was measured with a

298 plate reader (BMGLabtech, ClarioStar; excitation at 360 nm and emission at 460 nm). Quenched standard

299 curves were built to each sample separately on 4-methylumbelliferone (MU), and 7-amino-4-methylcoumarin

300 (AMC) for leucine amino-peptidase, by adding the same volume of soil slurry to each standard as was used in

301 the enzyme activity assay. Enzymatic activities were expressed as nmol of MU/AMC per g^{-1} soil DW h^{-1}.

302 Additionally, we measured oxidative enzymes (phenol oxidase EC 1.14.18.1 and peroxidase EC 1.11.1.x)

303 according to (Marx et al., 2001). A reaction mixture was prepared by adding 1 ml of soil suspension (prepared

304 as above) to 1 ml of 20 mM DOPA solution (L-3,4-dihydroxyphenylalanin) in sodium acetate buffer (100 mM,

305 pH 5.5). As a negative control, 1 ml of sodium acetate buffer and 1 ml of 20 mM DOPA solution were mixed;

306 as blanks, 1 ml of sodium acetate buffer was mixed with 1 ml of soil suspension. Samples and blanks were

307 shaken for 10 min and centrifuged (5 min, 2000g). Then, 250 µl of supernatants were dispensed into 96-well

308 microplates. For peroxidase activity measurement, 10 µl of 0.3% H_2O_2 was added. After measurement of initial

309 absorbance (450nm), plates were incubated in darkness for 20 hours at 20°C, and absorption was measured

310 again. Enzymatic activities were expressed as nmol of DOPA g^{-1} soil DW h^{-1}.

311

312 2.7 Soil + understorey respiration

313   At a distance of 50 cm from each tree or plot center, we drilled a PVC collar (22 cm diameter) into the soil one

314   week before the first measurement, by cutting roots and the organic layer with a knife, if necessary.

315   We measured soil + understorey respiration four times during July to September 2019. Soil + understorey

316   respiration in this study is defined as the sum of microbial, root, and understorey vegetation respiration. We

317   define the results as soil + understorey respiration – not as ecosystem respiration – because aboveground

318   respiration of trees was excluded in the measurements.

319   We placed a dark chamber (20 cm diameter, 25 cm height) on top of the collar, equipped with a fan to ensure

320   ventilation. After closing the chamber, CO_2 concentration (ppm) was allowed to equilibrate for 1 minute. The

321   CO_2 concentration within the chamber was then recorded every minute for 5 minutes by a Vaisala GMP252

322   probe (Vaisala Oyj, Finland). The CO_2 accumulation rate (ppm min^{-1}) was calculated using a linear part of the

323   recorded data, and CO_2 efflux F was calculated by equation 5 where $\frac{dC}{dt}$ is the change in CO_2-concentration

324   across measurement time (ppm min^{-1}), P is atmospheric pressure (in hPa, available from the nearest

325   meteorological station in Nuorgam and adjusted for the ~100 m difference in elevation, Finnish Meteorological

326   Institute, 2020), R is the gas constant (8.314 J mol^{-1} K^{-1}), T is the measurement temperature in Kelvin inside

327   the chamber, V is the chamber volume in m^3 (0.009841m³), and A is the chamber area in m² (0.039761m²).

328    $$F(gCO_2\ cm^{-2}s^{-1}) = \frac{dC}{dt} \times \frac{P}{RT} \times \frac{V}{A} \times \frac{10^{-6}}{60} \times 44.01\frac{g}{mol} \quad \text{(equation 5)}$$

329   Respiration measurements of each site were completed within 2 h, such that the temperature and moisture

330   conditions were similar for all plots within a site. The order of plots per site was randomized. Measurements

331   of the three sites were taken within one day, except for the last measurement date when the duration of daylight

332   was not sufficient.

333

334   2.8 Statistics

335   We consider site as a block factor in ANOVA or random effect in linear mixed effect models, respectively.

336   We present treatment-specific mean values of the three sites in our figures. However, since the tree status

337   appears to have different effects on soil properties at the three independent sites, we also discuss some site-

338   specific differences, which are shown in the Supplementary material.

339   To investigate the effect of tree status on C stocks, C contents, and organic layer thickness, we used linear

340   mixed effect models for each soil layer (organic, E, B) separately, with tree status and distance to the tree as

341   fixed effects and plot ID nested in site as a random effect. We also tested for interactions. If the tree status

342   effect was significant, Tukey's honest significance test was applied to further investigate differences between

343   each tree status. Data were checked for normality of residuals by visual inspection of qqplots, and variance

344   homogeneity was tested with a Levene test. If assumptions were violated, the model was repeated on log- or

345   square-transformed data. As this did not change the overall result, and because linear mixed effect models have

346   been shown to be robust to moderate violations of distributional assumptions (Schielzeth et al., 2020), we

347   decided to keep the original model.

348   To compare the effect of tree status on overall SOC stocks within a 1 m radius around the tree or plot center,

349   we multiplied the SOC stock (kg m²) at each distance with the area of the respective distance radius and

350   summed them. This was done for each soil layer separately, as well as for total SOC stocks. We performed a

351   one-way ANOVA with block design (site as block) and interaction term (tree status x site) for each soil layer

352   separately (i.e., organic layer, E horizon, B horizon), as well as for total SOC stocks. Data were checked for

353   normality of residuals with a Shapiro-Wilk test, and variance homogeneity was tested with a Levene test. If

354   data were not normally distributed or did not reveal homogeneity of variances, they were log- or square-

355   transformed.

356   To test for differences in soil + understorey respiration between tree statuses, we performed a linear mixed

357   effect model with tree status, measurement date, soil temperature, and soil moisture as fixed effects, and plot

358   ID nested in site as a random effect. We also tested for interactions. Non-significant interactions terms were

359   removed from the model in a stepwise manner. Tukey's honest significance test was applied to further

360   investigate differences between each tree status.

361   To test for differences in biochemical soil properties between tree statuses, we performed a one-way ANOVA

362   with block design (site as block) for each soil layer (organic, mineral) separately. If effects were significant, a

363 post hoc Tukey's honest significance test was applied. If data were not normally distributed or did not reveal

364 homogeneity of variances, they were log- or square-transformed.

365 Correlation analyses were conducted to explore relationships between the variables. In case of linear

366 relationships and normal distribution of data, Pearson's correlation coefficient was used. Otherwise,

367 Spearman's rank correlation coefficient was calculated.

368 Principal component analysis (PCA) was conducted to visualize relationships between the large number of

369 measured variables and differences between sites and tree statuses. PCA was performed for the organic layer

370 and mineral soil separately. All measured variables from the "process sample set" were included, except the

371 large number of measured enzymes, which showed no correlation with tree status. We further included the soil

372 + understorey respiration rate at the middle of the growing season (12 July). The PCAs were performed in R

373 using the function prcomp. Data were scaled to similar standard deviation and centered to a mean of zero.

374 Ellipses are presented at a confidence interval of 90%.

375 If not otherwise stated, we define significant differences as $p < 0.05$.

376 Statistics and figures were performed in R (version 3.6.1, R Core Team, 2013) and maps in ArcGIS (version

377 10.8, Esri).

378

379 **3. Results**

380 3.1 Understorey vegetation cover

381 Understorey vegetation was similar under living, dead$_{12}$, and dead$_{55}$ trees. The plant community of the treeless

382 tundra differed considerably from that under living and dead trees. In the treeless tundra, moss (*Dicranum*

383 *spp)*, lichen (*Ochrolechia frigida)*, and black crowberry (*Empetrum nigrum)* were most frequent, each covering

384 around 30% of the area. Other species occurred occasionally. Under living, dead$_{12}$, and dead$_{55}$ trees, *Empetrum*

385 *nigrum* accounted for 65–70% of the vegetation cover, i.e. a considerably higher percentage than in treeless

386 tundra. The remaining ~30% were mainly dominated by lingonberry (*Vaccinium vitis-idaea)*, *Dicranum spp*,

387 and *Ochrolechia frigida*, each accounting for ~10% of the area (supplementary material; Fig. S1).

388

389   3.2 Soil temperature and moisture

390   The VWC that was measured four times between the beginning of July and end of September was on average

391   higher at sites 2 and 3 in comparison with site 1, with significant differences in September but not in summer

392   (Table 1). There was no significant effect of tree status on VWC.

393   Soil temperature at a depth of 10 cm was significantly affected by tree status: soils under living trees had lower

394   average monthly temperatures in the summer compared with soil at the treeless tundra (Table 1). However,

395   during the winter months, soils under living trees were on average warmer than at the treeless tundra sites,

396   although this difference was not significant (Table 1, for details see also supplementary material; Fig. S2).

397   Hence, there was a significant tree status x month interaction (supplementary material; Table S1). At sites 1

398   and 3, summer temperatures under dead trees were intermediate between treeless tundra and living trees

399   (significant tree status x site effect). On average, the soil temperatures at site 3 were lower throughout the years

400   compared with site 1 and 2 (Table 1).

401

402   3.3 Above- and belowground carbon and nitrogen stocks

403   On average, the thickness of the organic layer was 5.5 ± 3.6 cm, but was significantly affected by tree status

404   and site (Table 2, Fig. 3 a). Both living and dead trees had thicker organic layers than the treeless tundra.

405   However, there was no consistent difference in organic layer thickness between living and dead trees: while

406   site 1 revealed decreasing organic layer thickness in the order of living>$dead_{12}$=$dead_{55}$>treeless, $dead_{55}$ trees

407   revealed the thickest organic layers at site 2 (Fig. S3). At site 3, organic layer thickness was generally lower,

408   with only small differences between tree status (Fig. S3). Differences between tree status persisted up to at

409   least 1 m from the tree, but decreased significantly with distance. Organic layer thickness did not change with

410   distance to the plot center in the treeless tundra plots, yielding a significant tree status x distance interaction.

411   C contents were also significantly higher under living and dead trees compared with the treeless tundra (Fig.

412   3 b). As a result, C stocks followed a similar pattern as organic layer thickness, with overall higher stocks

413   under living and dead trees compared with the treeless tundra. This effect similarly decreased with increasing

414   distance from the tree, and high variability between sites was seen (Fig. S3).

415 The average thickness of the E horizon was 2.1±0.8 cm across all sites, tree status, and distances from a tree.

416 The remaining mineral soil up to the bedrock ("B horizon") was on average 4.1±3.3 cm thick. In mineral soil,

417 neither the thickness, SOC contents nor SOC stocks were significantly different between tree statuses (Table

418 2). There was no clear trend with distance from the tree (Table 2, see also supplement material; Fig. S4 and

419 S4).

420 Total overall SOC stocks within 1 m distance (i.e. sum of SOC stocks from org+E+B, Fig. 4) decreased in the

421 order of $dead_{55}$>living>$dead_{12}$>treeless, with significant differences only between treeless tundra and living

422 trees and between treeless tundra and $dead_{55}$ (Fig. 4).

423 Overall ecosystem C stocks decreased in the order of living>$dead_{12}$>$dead_{55}$>treeless tundra (Fig. 4) and were

424 mainly driven by changes in aboveground biomass, which significantly decreased upon tree death, especially

425 at later stages.

426 Soil N stocks were also calculated (see supplementary information). Across all distances and sites, average N

427 stocks in the organic layer were 0.118±0.077 kg m² (living), 0.105±0.062 kg m² ($dead_{12}$), 0.130±0.084 kg m²

428 ($dead_{55}$), and 0.056±0.023 kg m² (treeless tundra). In the E layer, average N stocks were 0.078±0.035 kg m²

429 (living), 0.080±0.029 ($dead_{12}$), 0.087±0.040 kg m² ($dead_{55}$), 0.048±0.026 kg m² (treeless tundra). In the B layer,

430 average N stocks were 0.187±0.129 kg m² (living), 0.126±0.092 kg m² ($dead_{12}$), 0.150±0.133 kg m² ($dead_{55}$),

431 and 0.155±0.131 kg m² (treeless tundra). For site- and distance-specific N contents and N stocks, see Fig. S6,

432 S7, and S8.

433

434 3.4 Ex-situ soil respiration measurement

435 Basal respiration measured under standardized conditions of moisture (50% of WHC) and temperature (20°C)

436 decreased in the order of living>$dead_{12}$=$dead_{55}$> treeless tundra, both in the organic (Fig. 5a) and mineral layer

437 (Fig. 5f). The effect of tree status was significant in mineral soil, but only close to significant (p=0.09) in the

438 organic layer. A post-hoc test revealed significant differences in mineral soil only between living trees and the

439 treeless tundra (Fig. 5f). Although dead trees were not significantly different from living trees or the treeless

440 tundra, there was a tendency that dead trees were in transition between living trees and treeless tundra, both in

441 mineral soil and organic layer (Fig. 5a,f). The soil respiration rate was related to C contents in mineral soil

442 (r=0.55, p<0.001) but not in the organic layer (r=0.15, p=0.31). When expressed per g of C (i.e. SOC-specific

443 respiration), soil respiration was not significantly different between each tree status, neither in the organic layer

444 nor in the mineral soil (Fig. 5b,g). The SOC-specific respiration was inversely related to the C/N ratio in the

445 organic layer (r=-0.61, p<0.001) and mineral soil (r=-0.44, p<0.001).

446 Following the addition of glucose, hourly CO_2 release increased in comparison with basal respiration rate

447 (supplementary material; Fig. S9). The cumulative amount of CO_2 released within 100h after glucose addition

448 (i.e. SIR_{cum}) decreased in the order of living >$dead_{12}$=$dead_{55}$> treeless tundra, both in the organic layer (Fig.

449 5c) and in mineral soil (Fig. 5h). The effect of tree status was significant. Post-hoc tests revealed that SIR_{cum}

450 under living trees, $dead_{12}$, and $dead_{55}$ trees differed significantly from the treeless tundra in the organic layer.

451 In mineral soil, only living trees differed from the treeless tundra. There was a tendency for dead trees to differ

452 from living trees and from the treeless tundra, although these differences were not significant. SIR_{cum} was

453 positively related to the concentrations of NO_3, both in the organic layer (r=0.30, p=0.04) and in mineral soil

454 (r=0.35, p=0.02). Adding $(NH_4)_2SO_4$ to the glucose-amended mineral soil induced larger CO_2 release than

455 without N addition (supplementary material; Fig. S9).

456

457 3.5 Soil biological and chemical properties

458 Neither the pH value, C/N ratios, nor enzyme activities differed significantly between tree status (Table 3).

459 Moreover, the microbial biomass (MBC) did not differ significantly between tree status in the organic layer

460 and mineral soil (Fig. 5d,i), although there was a decreasing trend in the order of living>$dead_{55}$>$dead_{12}$>treeless

461 tundra (Fig. 5i).

462 Soil N availability differed across tree status: in the organic layer, NO_3^- concentrations were significantly

463 higher under living trees than under $dead_{55}$ and the treeless tundra; $dead_{12}$ was intermediate, although these

464 differences were not significant (Fig. 5e). This difference did not persist in mineral soil, where no significant

465 differences were found due to the overall low NO_3^- content (Fig. 5j). In all plots, NH_4^+ dominated the soil

466   mineral N pool with a minimum of 80% (Table 3), but did not differ significantly between tree status, neither

467   in the organic layer nor in mineral soil.

468

469   3.6 Soil+understorey respiration

470   Soil+understorey respiration was significantly higher under living and dead trees compared with the treeless

471   tundra, but there was no significant difference between living and dead trees (Table 4, Fig. 6). Nevertheless,

472   there were remarkable difference between tree status among the three sites (Fig. S10). At site 1 and site 3,

473   average soil+understorey respiration decreased in the order of living>$dead_{12}$>$dead_{55}$>treeless tundra. However,

474   at site 2, $dead_{55}$ revealed the highest ecosystem respiration rates, even exceeding those of living trees.

475

476   3.7 Principal component analysis

477   In the organic layer, the first and second principal components explained 29% and 25% of variance,

478   respectively (Fig. 7a). PC1 was significantly correlated ($p<0.05$) with the original variables: thickness of the

479   organic layer (r=-0.87), SOC stock (r=-0.85), C contents (r=-0.89), C/N ratio (r=-0.70), and SOC-specific

480   respiration (r=0.75), i.e. with variables related to SOC quantity and quality. PC2 was significantly correlated

481   with NO_3^- (r=-0.48), NH_4^+ (r=-0.36), N (r=-0.62), MBC (r=-0.70), SIR_{cum} (r=-0.88), soil + understorey

482   respiration (r=-0.45), and soil respiration (r=-0.89), i.e. with variables related to N availability and microbial

483   activity. Soil from treeless tundra was separated from living trees mainly along PC2, where treeless tundra

484   revealed higher values, i.e. lower N availability and microbial activity than living trees. Dead trees were

485   intermediate between living trees and treeless tundra. The soil properties in treeless tundra mainly varied along

486   the second component, whereas living trees varied along the first component, i.e. the PCA ellipse showing the

487   90% confidence interval of living trees was at a 45° angle to the ellipse of dead trees (Fig. 7a), which were

488   also immediate here. Further, living and dead trees revealed larger variability in the multidimensional space,

489   while treeless tundra clustered in a smaller area.

490   In mineral soil, the first and second principal components explained 34% and 19% of variance, respectively

491   (Fig. 7b). There was no clear clustering by tree status. As already observed for the organic layer, living trees

492   revealed the largest variability in the multidimensional space, while treeless tundra clustered in a smaller area,

493   with dead trees in between.

494

495   **4. Discussion**

496   In this study, we aimed to understand the effect of treeline advance and decline on SOC stocks and dynamics.

497   To this end, we compared SOC stocks and biochemical soil properties under living trees, treeless tundra, and

498   two stages of dead trees (12 and 55 years since moth outbreak) in a small-scale space-for-time approach. In

499   summary, our first hypothesis (section 4.1) of living trees having lower C stocks compared to treeless tundra

500   was rejected. Contrary to our hypothesis, the net effect of the living tree on soil C stocks was positive.

501   However, this does not exclude the possibility that the living tree enhances SOM decomposition via priming

502   effects. In fact, some of our results point towards higher priming effects under living trees, but the net effect

503   of the tree was positive, which means that the C losses from accelerated SOM decomposition under living trees

504   did not exceed the C inputs. Our second hypothesis (section 4.2) was that tree death causes the C stocks to

505   develop towards the C stocks of the treeless tundra. Indeed, several soil properties under dead trees were in

506   transition between those of living trees and treeless tundra. Yet, this did not apply to SOC stocks, which

507   remained at an elevated level comparable to that of living trees, even 55 years after the moth outbreak. Hence,

508   also our second hypothesis was rejected.

509

510   **4.1 Effect of living birch trees on ecosystem carbon stocks and soil organic matter turnover**

511   Assuming that priming is a relevant mechanism under living trees, we hypothesized that accelerated SOC

512   turnover leads to smaller SOC stocks under living trees compared to treeless tundra (Hartley et al., 2012; Parker

513   et al., 2015; Wilmking et al., 2006). Contrary to this hypothesis, we found that SOC stocks were on average

514   significantly higher under living trees compared with treeless tundra (Fig. 3c). Higher SOC stocks were still

515   evident even 1 m from the tree, although these differences decreased with increasing distance. Most studies

516   that have reported lower SOC stocks under living trees have compared forested sites with separate treeless

517   sites, e.g. along latitudinal or altitudinal transects or at locations with considerable distance between each other.

518 In such approaches, SOC stocks could be also affected by differences in temperature, moisture conditions, soil

519 characteristics and/or above- and belowground litter input (e.g. Rapalee et al., 1998; Sjögersten & Wookey,

520 2004). In this regard, a causal link between trees and lower SOC stocks is not certain. With our single tree

521 scale approach, we could investigate the effect of trees under otherwise rather similar conditions. Based on a

522 similar approach, Friggens et al. (2020a) identified decreasing SOC stocks with increasing distance from trees,

523 and thus a positive effect of trees on SOC stocks. Similarly, Adamczyk et al. (2019) showed that priming-

524 induced SOC losses are smaller than the positive effect of tree roots on SOC formation and stabilization. It

525 therefore seems likely that living trees can also accumulate SOM in subarctic soils, i.e. that trees have a positive

526 net effect on SOC stocks. Together with the large aboveground C storage shown here (Fig. 4) and elsewhere

527 (Heliasz et al., 2011), our results imply that living trees could strengthen the C sink of the ecosystem.

528 The effect of living trees on SOC stocks decreased with soil depth. Even if the average SOC stocks in the E

529 and B horizon were higher under living trees compared with treeless tundra (Fig. 4), this difference was not

530 statistically significant considering the large variability (Table 2, supplementary material; Fig S3 and S4).

531 Thus, the significant differences in SOC stocks between living trees and treeless tundra (Fig. 4) were mainly

532 driven by the thickness and C concentrations of the organic layer. It is surprising that the effect of living trees

533 does not persist with depth, as Ding et al. (2019) observed 46% of birch fine root biomass was located in

534 mineral soil, which may lead to considerable C inputs. It is possible that priming effects by root exudates

535 resulted in faster mineralization of SOM in the N-poor mineral soil under living trees. Hartley et al. (2010),

536 Karhu et al. (2016), and Wang et al. (2015) also found that positive priming mainly takes place in the mineral

537 soil, but not or at lower rates in the organic layer. Hence, the effect of higher SOC input under living trees may

538 be cancelled out by priming in mineral soil.

539 There is plenty of evidence from literature that priming effects occur in the field under living trees

540 (Clemmensen et al., 2021; Hartley et al., 2012; Parker et al., 2015. Adamczyk et al., 2019), and even though

541 we did not directly measure priming, we have several results that point towards accelerated SOM

542 decomposition under living trees at our sites, discussed in detail below.

543 Since priming is notoriously difficult to measure under field conditions, it is often investigated in incubation

544 experiments after the addition of ^{13}C labeled glucose, which allows native SOC mineralization to be

545   distinguished from mineralization of labile C (Karhu et al., 2016). Such experiments only indicate a potential

546   priming effect under standardized C supply, but do not reflect the naturally occurring priming intensity in soil

547   where labile C supply varies between living trees, dead trees, and treeless tundra. Yet, priming has been

548   reported to be driven by microbial N mining, i.e. by microbial decomposition of SOM for N acquisition (Chen

549   et al., 2014; Fontaine et al., 2011). In this context, Bengtson et al. (2012) and Dijkstra et al. (2009) pointed out

550   that N mineralization and priming are coupled: labile C supply (e.g. from fresh litter and root exudates)

551   increases microbial N demand, eventually increasing the activity of extracellular enzymes that decompose

552   SOM for N acquisition. Hence, mineral N contents may provide hints for priming. Indeed, we found higher

553   NO_3^- contents under living trees compared with treeless tundra. The finding of higher N availability under

554   living trees was also corroborated by incubation experiments after adding glucose: soils taken under living

555   trees were able to mineralize larger amounts of glucose, which, according to Nordgren (1992) and Meyer et

556   al. (2018) suggests higher amounts of available nutrients, in this case N (as tested by N additions,

557   supplementary material; Fig. S9). The finding that living birch trees increase soil N availability has also been

558   shown by Mikola et al. (2018) and Silfver et al. (2020). We interpret this finding as an indicator of N mining,

559   which is presumably coupled with accelerated turnover of SOM, i.e. with priming. However, higher mineral

560   N contents may also be interpreted inversely: higher mineral N contents under living trees may indicate less

561   need of microbes to decompose SOM for N acquisition (Craine et al., 2007), i.e. it suppresses priming. In light

562   of the very N-poor subarctic soils (Hicks et al., 2020), it seems contradictory to find an excess of mineral N

563   despite the greater N demand of birch roots. Hence, the excess of mineral N under living trees most likely

564   results from accelerated SOM decomposition close to the tree. This is further indicated by largest

565   soil+understorey respiration rates and microbial biomass under living trees.

566

567   Besides higher mineral N contents, we also found elevated N stocks under living trees than under treeless

568   tundra. As both C and N are major components of SOM, higher N stocks under living trees are not necessarily

569   surprising, since SOC stocks were also high. In such nutrient limited regions, it is unlikely that the soil beneath

570   the tree contained sufficient N for accumulating such high amounts of above- and belowground organic matter

571   stocks. While larger mineral N contents can be explained by accelerated SOM decomposition close to the tree,

another mechanism must be responsible for elevated N stocks. Although N fixation might be a potential source of N (Rousk & Michelsen, 2017), we do not think that this can explain the excess of N under living trees, especially because mosses as important N fixing species (Zackrisson et al., 2009) are more abundant in the treeless tundra (Fig. S1). Notably, birch trees form symbioses with ectomycorrhizal (ECM) fungi that can extend their hyphae several meters (Simard & Durall, 2004) while "mining" the soil for N by decomposing SOM. Friggens et al. (2020a) also highlight ectomycorrhizal networks of birch trees that exploit resources throughout a forest. In this context, ECM fungi were reported to stimulate organic matter decomposition (Clemmensen et al., 2021) and hence, to be critically involved in priming (Paterson et al., 2016; Read & Perez-Moreno, 2003). As a result, litterfall concentrates N that has been acquired from a larger volume of soil, to a smaller area around it. Hence, elevated N stocks below the tree may indeed be indicative of N mining, a process which has also been observed in other mountain birch forests in Fennoscandia (Clemmensen et al., 2021). Yet, locations of excess N stocks do not necessarily match locations where N was mined and the associated priming took place. We suggest that N mining and priming are not exclusively coupled in a spatial way and hypothesize that elevated N stocks, in parts, could originate from SOM decomposition further away from the tree.

We found further indications that priming-induced SOC losses can be considerable, even if this was on average not the case in our study area. Our results revealed considerable variations in SOC stocks and dynamics between the three investigated sites (supplementary material; Fig. S3). The finding that site 3 had low SOC stocks under living trees was remarkable, as tree biomass and thus C input to soil was largest compared with the other sites. Also, respiration rates under living trees were at a similar or even higher level at site 3 compared with the other sites (Fig. S10), even though site 3 was characterized by lower SOC stocks, similar potential SOC decomposability, and colder temperatures. Hence, root respiration may have a higher contribution to soil + understorey respiration at site 3 than in other sites. The amount of root respiration is correlated with the amount of root exudation (Sun et al., 2017), which is one of the main C sources that cause priming (Shahzad et al., 2015). Hence, it can be speculated that larger priming effects are responsible for the low SOC stocks under living trees at site 3. Thus, we suggest that in some cases the high amount of N required by large trees can stimulate SOM decomposition to such an extent that it compensates for elevated SOC inputs (cf. Hartley et al., 2012), making it noteworthy to conduct these studies on several independent sites simultaneously.

599 Further, differences in understorey vegetation may obscure the relevance of priming-induced SOC losses under

600 living trees. The species composition of understorey vegetation differed significantly between living trees and

601 treeless tundra, likely as a result of differences in nutrient supply. Living trees were associated with larger

602 proportions of dwarf shrubs, while treeless tundra was associated with moss and lichen. Also Ylänne et al.

603 (2021) reported a significantly higher proportion of *Vaccinium* sequence reads and higher soil OM content in

604 samples collected from vicinity of mountain birches than samples collected further away from the trees. We

605 could confirm their observation based on the vegetation mapping in our study. It has been reported that C input

606 by the understorey vegetation can make a substantial contribution to total soil C input in forests, especially in

607 the north. For instance, Liski et al. (2006) estimated that understorey vegetation accounts for an average of

608 28% of C input across a range of different forest types in Finland. The importance of the understorey vegetation

609 may be even greater when exclusively focusing on subarctic birch forests, e.g. 35% according to Ding et al.

610 (2019). Hence, the dwarf shrub dominated understorey vegetation may contribute to the observed

611 accumulation of SOC under living trees, especially in the organic layer where 80% of understorey root biomass

612 is located (Ding et al., 2019). The finding of greater understorey root biomass under living trees in comparison

613 with treeless tundra supports this assumption (Fig. 4). Hence, the understorey vegetation may obscure the

614 direct effect of trees on SOC stocks, i.e. the magnitude of accelerated SOC turnover by birch trees may be

615 underestimated.

616 Overall, living trees increased the heterogeneity of SOM stocks and dynamics in comparison with treeless

617 tundra. The PCA plot indicates that the treeless tundra clusters in a narrower range in the multidimensional

618 space compared to living trees. This was especially true for mineral soil, where treeless tundra revealed little

619 variation. We assume that differences in tree properties (e.g. age, size, root system, etc.) induce a different

620 degree of priming, N mineralization, and SOC accumulation. This has also been shown by Friggens et al.

621 (2020a), suggesting large variations in respiration and mycorrhizosphere productivity between studied trees.

622 Thus, we conclude that trees generate soil heterogeneity, ultimately increasing patchiness of subarctic

623 landscapes.

624

625 **4.2 Effect of dead trees on ecosystem carbon stocks and soil organic matter turnover**

626   We originally hypothesized that tree death causes the soil C stocks under the tree to develop towards the C

627   stocks of the treeless tundra, i.e. to be in transition between living trees and treeless tundra. Contrary to our

628   expectations, we did not find a consistent development back to tundra-like SOC stocks within 55 years after

629   tree death, i.e. SOC stocks under dead trees did not significantly differ from those under living trees. In a short-

630   term study, Sandén et al. (2020) also found no change in SOC stocks within 8 years after tree death. Similarly,

631   no change in SOC stocks was found within 4 years after tree death in boreal *Picea abies* stands caused by a

632   bark beetle outbreak (Kosunen et al., 2020). A continual supply of decaying wood seems to maintain SOC

633   stocks at comparatively high levels, even decades after tree dieback.

634   In addition to continual supply of decaying wood, elevated SOC stocks under dead trees in comparison with

635   treeless tundra may be further explained by the understorey vegetation. Karlsen et al. (2013) and Sandén et al.

636   (2020) reported that moth outbreaks affect the understorey vegetation towards a grass dominated community

637   with consequently labile litter input to soils. We could not confirm this observation in our study, possibly

638   because the appearance of grasses is a short-lived effect caused by the sudden nutrient supply during and

639   shortly after an outbreak event (Vuojala-Magga and Turunen, 2015). Here, the understorey community

640   remained unaffected by tree death and resembled that of living trees. Thus, the amount of soil C inputs from

641   understorey litter and roots may be similar under living and dead trees, but clearly different from treeless

642   tundra. This can be of quantitative relevance: according to Liski et al. (2006), the understorey vegetation was

643   estimated to account for 26% of the total soil C inputs in Finnish forests. This contribution may be even higher

644   in northern birch forests, i.e. 35% according to Ding et al. (2019). Moreover, the composition of SOM may be

645   dominated by recalcitrant litter input from *Empetrum nigrum* (Tybirk et al., 2000), both under living and dead

646   trees, eventually resulting in accumulation of SOM. The combination of ongoing deadwood supply and

647   unaltered C input from understorey vegetation may partly explain the unaltered SOC stocks upon tree death.

648   A further explanation for the unchanged SOC stocks may be a slowed SOM decomposition, which can be

649   assumed for several reasons. First, quality of SOM may change towards a larger proportion of recalcitrant

650   compounds once the most labile compounds of decaying wood have been mineralized (Mackensen and

651   Bauhus, 2003). This, however, was not observed here. Instead, the SOC-normalized respiration did not

652   decrease upon tree death, which indicates similar potential decomposability of SOC under living and dead

653   trees (Fang & Moncrieff, 2005; Mikan et al., 2002). This finding may be partly explained by the unchanged

654   understorey vegetation (see above), thereby attenuating the effect of tree death on overall SOC

655   decomposability. Second, the need of vegetation and microorganisms for N may decrease in the absence of

656   trees, tree exudates (Bengtson et al., 2012) and mycorrhiza (Paterson et al., 2016; Read & Perez-Moreno,

657   2003). Together with the excess of available N in the soil both before (i.e. living trees, Fig. 5) and immediately

658   after the moth outbreak event (Kaukonen et al., 2013), N deficiency was likely alleviated after tree death,

659   which may restrict SOM decomposition for the N acquisition, i.e. N mining. Indeed, we found lower NO_3

660   contents and SIR_{cum} under dead trees compared with living trees, which points to smaller amounts of available

661   nutrients. This indicates that SOM turnover – but not potential decomposability of SOM – decreased upon tree

662   death. Lower soil + understorey respiration and MBC under dead trees compared with living trees further

663   support this assumption. In summary, the combination of ongoing deadwood supply, unaltered C input from

664   understorey vegetation, and slowed SOM turnover may explain why SOC mineralization could not exceed

665   SOC input for at least 55 years after tree death.

666   Our results of lower N availability, MBC, and soil respiration under dead trees oppose previous observations

667   that mainly covered the short-term effects of moth outbreaks. Such studies mainly referred to the deposition

668   of insect frass, which was reported to be more easily available to microbes than senesced litter (Kristensen et

669   al., 2018), thereby enhancing SOM turnover (Kaukonen et al., 2013). Increases in available N and dissolved

670   organic carbon were also reported, with stimulating effects on MBC and ultimately soil respiration (Kaukonen

671   et al., 2013; Kristensen et al., 2018; Sandén et al., 2020). Here, we did not observe any of these short-term

672   effects that have been observed after moth outbreaks, neither after 12 nor 55 years since the outbreak. This

673   contradiction to previous studies is likely a result of the different time scale considered. Kristensen et al. (2018)

674   speculated that moth outbreaks cause a short-term increase, but long-term decrease in decomposition rates of

675   SOM. Hence, the stimulation of microbial activity upon tree death is likely a short-lived effect triggered by a

676   sudden C and N supply that is not reflected in our data.

677   Although we found indications for decreasing SOM turnover under dead trees, it did not reach the level of

678   treeless tundra, even after 55 years. Enzyme activities reflect unaltered C or N acquisition strategies of soil

679   microbes upon tree death. Indeed, leaching of dissolved organic carbon from deadwood has been reported,

680 thereby stimulating MBC and respiration (Bantle et al., 2014; Peršoh & Borken, 2017). This effect may persist

681 in the long-term. For instance, Minnich et al. (2020) observed elevated MBC and SOC mineralization rates in

682 soil beneath deadwood even 8 years after experimentally placing logs on the forest floor. Further, several

683 studies showed that fungi transfer N from soil to the decaying wood (Philpott et al., 2014; Rinne et al., 2017;

684 Oleveira Longa et al., 2018), hence N mining may continue upon tree death. Such processes may likely be

685 more prominent in our long-term study with more deadwood laying on the forest floor compared to studies

686 that focused on short-term effects of moth outbreaks with standing trees. Hence, N mining and associated

687 priming may continue for a long time after tree death, although at lower rates, and mainly triggered by

688 deadwood instead of root exudates as a source of labile C. This transitional state of dead trees is also visualized

689 by the PCA. In the organic layer, living trees clustered in the lower part of the plot, while treeless tundra was

690 on the upper part and dead trees were in between (Fig. 7a). Hence, tree death is accompanied by a transition

691 from a rather N-rich soil with high microbial activity to a N-poor soil with low microbial activity. These

692 changes in soil properties upon tree death indicate a shift in characteristics of biogeochemical cycling towards

693 a state comparable with treeless tundra. Yet, even after 55 years, SOM turnover was still elevated in

694 comparison to treeless tundra.

695 While SOC stocks remained at an elevated level even decades after moth outbreaks, it should be highlighted

696 that the overall ecosystem carbon stock was clearly reduced by tree death, mainly caused by a decline in

697 aboveground biomass. In such heavily grazed areas, reindeer grazing is a crucial factor in regulating birch

698 growth (Stark et al., 2021), thereby possibly also determining whether birch trees recover or die after moth

699 defoliation (Lehtonen & Heikkinen 1995). It may also restrict growth of new trees (Biuw et al., 2014; Olofsson

700 et al., 2009). There is clear evidence from published studies that regeneration of birch forest is hampered on

701 the year-round grazed areas on the Finnish side, compared to Norway, where the reindeer migrate seasonally

702 between summer and winter range (Biuw et al., 2014; Kumpula et al., 2011). While the long-term trends in

703 reindeer population densities are quite similar in both countries, the overall reindeer densities in Norway (1.56

704 reindeer/km² in 2006/2007) are slightly lower than in our study area (2.38 reindeer/km² in 2006/2007; Biuw et

705 al., 2014). Moreover, seasonal migration of reindeer is still practiced in the neighbored areas in Norway, i.e.

706 there are separate seasonal pastures with summer grazing in coastal areas, and only winter grazing (i.e. no

707 grazing on birches) in the interior birch forests. In our study area, in contrast, the area is a year-round pasture

708 for reindeer (Biuw et al., 2014). However, it remains uncertain to what extent the lack of forest recovery on

709 our sites was affected by reindeer densities and on the other hand by historical developments in the study area,

710 preventing the reindeer from going into separate summer and winter pastures. In the circumpolar Arctic, it is

711 more common for the reindeer to migrate seasonally between winter and summer ranges (Stark et al., 2021),

712 which affects the generalization of our findings over a larger geographical scale. In summary, we conclude

713 that in this area, the increased occurrence of moth damage would have minor effects on SOC stocks, but would

714 decrease ecosystem C stocks if the mountain birch forests will not be able to recover from the outbreaks.

715 However, we cannot exclude the possibility that the effect of moth outbreaks on ecosystem C stocks are

716 different in regions that are less heavily affected by grazing, which calls for a comparison of areas with

717 different grazing intensities.

718

719 **Conclusions**

720 Our results indicate that trees strengthen the subarctic carbon sink in the Pulmankijärvi area of Finnish Lapland

721 by increasing above- and belowground carbon stocks. Forest dieback by severe moth damage may become

722 more frequent in the future due to climate change, and may decrease the total ecosystem C stocks. However,

723 although aboveground biomass decreases upon tree death, SOC stocks under dead trees remained at

724 comparable levels to living trees for at least 55 years. We conclude that a CO_2-related positive feedback of

725 forest disturbance on climate change might be small and very slow in subarctic region, although only with

726 respect to soil, but not aboveground stocks. Importantly, our data also highlight considerable spatial variability

727 in the effect of tree status on SOC stocks. This clearly warns against comparing separate sites of living forests,

728 dead forests, and treeless tundra when making predictions about the effect of treeline advancement or

729 recession. We consider the small-scale approach as a more reasonable space-for-time substitution in such

730 patchy landscapes. While our study represents a comprehensive survey of the net effects of mountain birch

731 tree deaths on ecosystem soil C stocks in the Pulmankijärvi area, similar small-scale studies are required in

732 other regions of Fennoscandia to study how generalizable our findings are.

733

References

Adamczyk, B., Sietiö, O.-M., Straková, P., Prommer, J., Wild, B., Hagner, M., Pihlatie, M., Fritze, H., Richter, A., Heinonsalo, J., 2019. Plant roots increase both decomposition and stable organic matter formation in boreal forest soil. Nature Communications 10, 3982. https://doi.org/10.1038/s41467-019-11993-1

Ali, R.S., Kandeler, E., Marhan, S., Demyan, M.S., Ingwersen, J., Mirzaeitalarposhti, R., Rasche, F., Cadisch, G., Poll, C., 2018. Controls on microbially regulated soil organic carbon decomposition at the regional scale. Soil Biology and Biochemistry 118, 59-68. https://doi.org/10.1016/j.soilbio.2017.12.007

Anderson, J.P.E., Domsch, K.H., 1978. A physiological method for quantitative measurement of microbial biomass in soils. Soil Biology and Biochemistry 10, 215-221. https://doi.org/10.1016/0038-0717(78)90099-8.

Bantle A., Borken W., Ellerbrock R.H., Schulze, E.D., Weisser, W.W., Matzner, E., 2014. Quantity and quality of dissolved organic carbon released from coarse woody debris of different tree species in the early phase of decomposition. Forest Ecology and Management 329, 287-94. https://doi.org/10.1016/j.foreco.2014.06.035

Bell, C.W., Fricks, B.E., Rocca, J.D., Steinweg, J.M., McMahon, S.K., Wallenstein, M.D., 2013. High-throughput fluorometric measurement of potential soil extracellular enzyme activities. Journal of Visualized Experiments 81, e50961. https://doi.org/10.3791/50961

759   Bengtson, P., Barker, J., Grayston, S.J., 2012. Evidence of a strong coupling between root exudation, C and

760   N availability, and stimulated SOM decomposition caused by rhizosphere priming effects. Ecology and

761   Evolution 2(8), 1843-1852. https://doi.org/10.1002/ece3.311

762   Biuw, M., Jepsen, J.U., Cohen, J., Ahonen, S.H., Tejesvi, M., Aikio, S., Wäli, P.R., Vindstad, U.P.L.,

763   Markkola, A., Niemelä, P., Ims, R.A., 2014. Long-term impacts of contrasting management of large

764   ungulates in the arctic tundra-forest ecotone: Ecosystem structure and climate feedback. Ecosystems 17, 890-

765   905. https://doi.org/10.1007/s10021-014-9767-3

766   Blagodatsky, S., Heinemeyer, O. & Richter, J., 2000. Estimating the active and total soil microbial biomass

767   by kinetic respiration analysis. Biology and Fertility of Soils 32, 73–81.

768   https://doi.org/10.1007/s003740000219

769   Dahl, M.B., Priemé, A., Brejnrod, A., Brusvang, P., Lund, M., Nymand, J., Kramshøj, M., Ro-Poulsen, H.,

770   Haugwitz, M.S., 2017. Warming, shading and a moth outbreak reduce tundra carbon sink strength

771   dramatically by changing plant cover and soil microbial activity. Scientific Reports 7, 16035.

772   https://doi.org/10.1038/s41598-017-16007-y

773   Carter, M.R., Gregorich, E.G., 2008. Soil Sampling and Methods of Analysis. 2nd. Taylor & Francis Group,

774   CRC Press.

775   Chen, R., Senbayram, M., Blagodatsky, S., Myachina, O., Dittert, K., Lin, X., Blagodatskaya, E. and

776   Kuzyakov, Y., 2014. Soil C and N availability determine the priming effect: microbial N mining and

777   stoichiometric decomposition theories. Global Change Biology 20, 2356-2367.

778   https://doi.org/10.1111/gcb.12475

779   Chen, Y., Liu, Y., Zhang, J., Yang, W., He, R., Deng, C., 2018. Microclimate exerts greater control over

780   litter decomposition and enzyme activity than litter quality in an alpine forest-tundra ecotone. Scientific

781   Reports 8, 14998. https://doi.org/10.1038/s41598-018-33186-4

782   Christensen, T.R., Johansson, T., Olsrud, M., Ström, L., Lindroth, A., Mastepanov, M., Malmer, N., Friborg,

783   T., Crill, P., Callaghan, T.V., 2007. A catchment-scale carbon and greenhouse gas budget of a subarctic

784   landscape. Philosophical Transactions of the Royal Society A 365(1856), 1643-1656.

785   https://doi.org/10.1098/rsta.2007.2035

786   Clemmensen, K.E., Durling, M.B., Michelsen, A., Hallin, S., Finlay, R.D., Lindahl, B.D., 2021. A tipping

787   point in carbon storage when forest expands into tundra is related to mycorrhizal recycling of nitrogen.

788   Ecology Letters 24, 1193–1204. https://doi.org/10.1111/ele.13735Craine, J.M., Morrow, C., Fierer, N., 2007.

789   Microbial nitrogen limitation increases decomposition. Ecology 88(8), 2105-2113.

790   https://doi.org/10.1890/06-1847.1

791   Dijkstra, F.A., Bader, N.E., Johnson, D.W., Cheng, W., 2009. Does accelerated soil organic matter

792   decomposition in the presence of plants increase plant N availability? Soil Biology and Biochemistry 41(6),

793   1080-1087. https://doi.org/10.1016/j.soilbio.2009.02.013.

794   Dijkstra, F.A., Carrillo, Y., Pendall, E., Morgan, J.A., 2013. Rhizosphere priming: a nutrient perspective.

795   Frontiers in Microbiology 4, 216. https://doi.org/10.3389/fmicb.2013.00216

796   Ding, Y., Leppälammi-Kujansuu, J., Helmisaari, H.-S., 2019. Fine root longevity and below- and

797   aboveground litter production in a boreal Betula pendula forest. Forest Ecology and Management 431, 17-25.

798   https://doi.org/10.1016/j.foreco.2018.02.039.

799   Fang, C., Moncrieff, J.B., 2005. The variation of soil microbial respiration with depth in relation to soil

800   carbon composition. Plant and Soil 268, 243-253. https://doi.org/10.1007/s11104-004-0278-4

801   Fenner, M., 1997. Evaluation of methods for estimating vegetation cover in a simulated grassland sward.

802   Journal of Biological Education 31, 49-54. https://doi.org/10.1080/00219266.1997.9655532

803   Finnish meteorological institute (2020). https://en.ilmatieteenlaitos.fi/statistics-from-1961-onwards

804   Fontaine, S., Bardoux, G., Abbadie, L. and Mariotti, A., 2004. Carbon input to soil may decrease soil carbon

805   content. Ecology Letters 7, 314-320. https://doi.org/10.1111/j.1461-0248.2004.00579.x

806   Fontaine, S., Henault, C., Aamor, A., Bdioui, N., Bloor, J.M.G., Maire, V., Mary, B., Revaillot, S., Maron,

807   P.A., 2011. Fungi mediate long term sequestration of carbon and nitrogen in soil through their priming

808   effect. Soil Biology and Biochemistry 43(1), 86-96. https://doi.org/10.1016/j.soilbio.2010.09.017

809   Friggens, N.L., Aspray, T.J., Parker, T.C., Subke, J.-A., Wookey, P.A., 2020a. Spatial patterns in soil

810   organic matter dynamics are shaped by mycorrhizosphere interactions in a treeline forest. Plant and Soil 447,

811   521-535. https://doi.org/10.1007/s11104-019-04398-y

812   Friggens, N.L., Hester, A.J., Mitchell, R.J., Parker, T.C., Subke, J.-A., Wookey, P.A., 2020b. Tree planting

813   in organic soils does not result in net carbon sequestration on decadal timescales. Global Change Biology 26,

814   5178-5188. https://doi.org/10.1111/gcb.15229

815   Hagen, S.B., Jepsen, J.U., Ims, R.A., Yoccoz, N.G., 2007. Shifting altitudinal distribution of outbreak zones

816   of winter moth Operophtera brumata in sub-arctic birch forest: a response to recent climate warming?

817   Ecography 30, 299-307. https://doi.org/10.1111/j.0906-7590.2007.04981.x

818   Hartley, I.P., Hopkins, D.W., Sommerkorn, M., Wookey, P.A., 2010. The response of organic matter

819   mineralisation to nutrient and substrate additions in sub-arctic soils. Soil Biology and Biochemistry 42(1),

820   92-100. https://doi.org/10.1016/j.soilbio.2009.10.004

821   Hartley, I., Garnett, M., Sommerkorn, M., Hopkins, D.W., Fletcher, B.J., Sloan, V.L., Phoenix, G.K.,

822   Wookey, P.A., 2012. A potential loss of carbon associated with greater plant growth in the European Arctic.

823   Nature Climate Change 2, 875-879. https://doi.org/10.1038/nclimate1575

824   Heräjärvi, H., 2004. Variation of basic density and brinell hardness within mature finnish Betula pendula and

825   B-pubescens stems. Variation of basic density and Brinell hardness within mature Finnish Betula pendula

826   and B. pubescens stems. Wood and Fiber Science 36, 216-227.

827   Heliasz, M., Johansson, T., Lindroth, A., Mölder, M., Mastepanov, M., Friborg, T., Callaghan, T.V.,

828   Christensen, T.R., 2011. Quantification of C uptake in subarctic birch forest after setback by an extreme

829   insect outbreak. Geophysical Research Letters 38(1). https://doi.org/10.1029/2010GL044733

830   Hinneri, S., Sonesson, M., Veum, A.K., 1975. Soils of Fennoscandian IBP Tundra Ecosystems. In:

831   Wielgolaski F.E. (eds), Fennoscandian Tundra Ecosystems. Ecological Studies (Analysis and Synthesis), vol

832   16. Springer, Berlin, Heidelberg. https://doi.org/10.1007/978-3-642-80937-8_2

833   Hicks, L.C., Leizeaga, A., Rousk, K., Michelsen, A., Rousk, J., 2020. Simulated rhizosphere deposits induce

834   microbial N-mining that may accelerate shrubification in the subarctic. Ecology.

835   https://doi.org/10.1002/ecy.3094

836   Hofgaard, A., Tømmervik, H., Rees, G., Hanssen, F., 2012. Latitudinal forest advance in northernmost

837   Norway since the early 20th century. Journal of Biogeography 40(5), 938-949.

838   https://doi.org/10.1111/jbi.12053

839   Huttunen, L., Niemelä, P., Ossipov, V., Rousi, M., Klemola, T., 2012. Do warmer growing seasons

840   ameliorate the recovery of mountain birches after winter moth outbreak? Trees 26, 809-819.

841   https://doi.org/10.1007/s00468-011-0652-9

842   ISO 17155:2012. Soil quality — Determination of abundance and activity of soil microflora using respiration

843   curves. ISO Secretariat, Geneva.

844   Jepsen, J.U., Hagen, S.B., Ims, R.A., Yoccoz, N.G., 2007. Climate change and outbreaks of the geometrids

845   Operophtera brumata and Epirrita autumnata in subarctic birch forest: evidence of a recent outbreak range

846   expansion. Journal of Animal Ecology 77(2), 257-264. https://doi.org/10.1111/j.1365-2656.2007.01339.x

847   Jepsen, J., Hagen, S., Høgda, K., Ims, R., Karlsen, S., Tømmervik, H., Yoccoz, N., 2009. Monitoring the

848   spatio-temporal dynamics of geometrid moth outbreaks in birch forest using MODIS-NDVI data. Remote

849   Sensing of Environment 113, 1939-1947.

850   Karhu, K., Hilasvuori, E., Fritze, H., Biasi, C., Nykänen, H., Liski, J., Vanhala, P., Heinonsalo, J.,

851   Pumpanen, J., 2016. Priming effect increases with depth in a boreal forest soil. Soil Biology and

852   Biochemistry 99, 104-107. https://doi.org/10.1016/j.soilbio.2016.05.001.

853   Karlsen, S.R., Jepsen, J.U., Odland, A., Ims, R.A., Elvebakk, A., 2013. Outbreaks by canopy-feeding

854   geometrid moth cause state-dependent shifts in understorey plant communities. Oecologia 173, 859-870.

855   https://doi.org/10.1007/s00442-013-2648-1

856   Kaukonen, M., Ruotsalainen, A.L., Wäli, P.R., Männistö, M.K., Setälä, H., Saravesi, K., Huusko, K.,

857   Markkola, A., 2013. Moth herbivory enhances resource turnover in subarctic mountain birch forests?

858   Ecology 94, 267-272. https://doi.org/10.1890/12-0917.1

859   Kosunen, K., Peltoniemi, K., Pennanen, T., Lyytikäinen-Saarenmaa, P., Adamczyk, B., Fritze, H., Zhou, X.,

860   Starr, M., 2020. Storm and Ips typographus disturbance effects on carbon stocks, humus layer carbon

861   fractions and microbial community composition in boreal Picea abies stands. Soil Biology and Biochemistry

862   148, 107853. https://doi.org/10.1016/j.soilbio.2020.107853

863   Köster, K., Metslaid, M., Engelhart, J., Köster, E., 2015. Dead wood basic density, and the concentration of

864   carbon and nitrogen for main tree species in managed hemiboreal forests. Forest Ecology and Management

865   354, 35-42. https://doi.org/10.1016/j.foreco.2015.06.039.

866   Krankina, O.N., Harmon, M.E., 1995. Dynamics of the dead wood carbon pool in northwestern Russian

867   boreal forests. Water, Air, and Soil Pollution 82, 227-238. https://doi.org/10.1007/BF01182836

868   Kristensen, J.A., Metcalfe, D.B., Rousk, J., 2018. The biogeochemical consequences of litter transformation

869   by insect herbivory in the Subarctic: a microcosm simulation experiment. Biogeochemistry 138, 323–336.

870   https://doi.org/10.1007/s10533-018-0448-8

871   Kumpula, J., Stark, S., & Holand, Ø., 2011. Seasonal grazing effects by semi-domesticated reindeer on

872   subarctic mountain birch forests. Polar Biology 34(3), 441–453. *https://doi.org/10.1007/s00300-010-0899-4*

873   Kuzyakov, Y., Friedel, J.K., Stahr, K., 2000. Review of mechanisms and quantification of priming effects.

874   Soil Biology and Biochemistry 32(11-12), 1485-1498. https://doi.org/10.1016/S0038-0717(00)00084-5.

875   Lehmann, J., Kleber, M., 2015. The contentious nature of soil organic matter. Nature 528, 60-68.

876   https://doi.org/10.1016/S0038-0717(00)00084-5

877   Lehtonen, J., Heikkinen, R.K., 1995. On the recovery of mountain birch after Epirrita damage in Finnish

878   Lapland, with a particular emphasis on reindeer grazing. Écoscience, 2(4), 349-356,

879   https://doi.org/10.1080/11956860.1995.11682303

880   Liski, J., Lehtonen, A., Palosuo, T., Peltoniemi, M., Eggers, T., Muukkonen, P., Mäkipää, R., 2006. Carbon

881   accumulation in Finland's forests 1922–2004 – an estimate obtained by combination of forest inventory data

882   with modelling of biomass, litter and soil. Annals of Forest Science 63(7), 687-697.

883   https://doi.org/10.1051/forest:2006049

884 Mackensen, J., Bauhus, J., 2003. Density loss and respiration rates in coarse woody debris of Pinus radiata,

885 Eucalyptus regnans and Eucalyptus maculata. Soil Biology and Biochemistry 35, 177-186.

886 https://doi.org/10.1016/S0038-0717(02)00255-9

887 Marx, M.C., Wood, M., Jarvis, S.C., 2001. A microplate fluorimetric assay for the study of enzyme diversity

888 in soils. Soil Biology and Biochemistry 33, 1633-1640. https://doi.org/10.1016/S0038-0717(01)00079-7

889 Meyer, N., Welp, G., Bornemann, L., Amelung, W., 2017. Microbial nitrogen mining affects spatio-temporal

890 patterns of substrate-induced respiration during seven years of bare fallow. Soil Biology and Biochemistry

891 104, 175-184. https://doi.org/10.1016/j.soilbio.2016.10.019

892 Meyer, N., Welp, G., Rodionov, A., Borchard, N., Martius, C., Amelung, W., 2018. Nitrogen and

893 phosphorus supply controls soil organic carbon mineralization in tropical topsoil and subsoil. Soil Biology

894 and Biochemistry 119, 152-161. https://doi.org/10.1016/j.soilbio.2018.01.024

895 Mikan, C.J., Schimel, J.P., Doyle, A.P., 2002. Temperature controls of microbial respiration in arctic tundra

896 soils above and below freezing. Soil Biology and Biochemistry 34(11), 1785-1795.

897 https://doi.org/10.1016/S0038-0717(02)00168-2

898 Mikola, J., Silfver, T., Rousi, M., 2018. Mountain birch facilitates Scots pine in the northern tree line–does

899 improved soil fertility have a role? Plant and Soil 423, 205-213. https://doi.org/10.1007/s11104-017-3517-1

900 Minnich, C., Peršoh, D., Poll, C., Borken, W., 2020. Changes in chemical and microbial soil parameters

901 following 8 years of deadwood decay: an experiment with logs of 13 tree species in 30 forests. Ecosystems.

902 https://doi.org/10.1007/s10021-020-00562-z

903 Miranda, K.M., Espey, M.G., Wink, D.A., 2001. A rapid, simple spectrophotometric method for

904 simultaneous detection of nitrate and nitrite. Nitric oxide 5, 62-71. https://doi.org/10.1006/niox.2000.0319

905 Moorhead, D. L., Sinsabaugh, R. L., 2006. A theoretical model of litter decay and microbial interaction.

906 Ecological Monographs 76, 151-174. https://doi.org/10.1890/0012-

907 9615(2006)076[0151:ATMOLD]2.0.CO;2

908 Neuvonen, S., Niemelä, P., Virtanen, T., 1999. Climatic change and insect outbreaks in boreal forests: the

909 role of winter temperatures. Ecological Bulletins 47, 63-67. https://www.jstor.org/stable/20113228

910   Nordgren A., 1988. Apparatus for the continuous long-term monitoring of soil respiration rate in large

911   numbers of samples. Soil Biology and Biochemistry 20, 955-958. https://doi.org/10.1016/0038-

912   0717(88)90110-1

913   Nordgren, A., 1992. A method for determining microbially available N and P in an organic soil. Biology

914   Fertility of Soils 13, 195-199. https://doi.org/10.1007/BF00340575

915   Nuorteva, P., 1963. The influence of Oporinia autumnata (Bkh.) (Lep., Geometridae) on the timberline in

916   subarctic conditions. Annales Entomologici Fennici 29, 270-277.

917   Oliveira Longa, C.M., Francioli, D., Gómez-Brandón, M., Ascher-Jenull, J., Bardelli, T., Pietramellara, G.,

918   Egli, M., Sartori, G., Insam, H., 2018. Culturable fungi associated with wood decay of Picea abies in

919   subalpine forest soils: a field-mesocosm case study. Forest 11, 781-5. https://doi.org/10.3832/ifor2846-011

920   Olofsson, J., Oksanen, L., Callaghan, T., Hulme, P.E., Oksanen, T. and Suominen, O., 2009. Herbivores

921   inhibit climate-driven shrub expansion on the tundra. Global Change Biology 15, 2681-2693.

922   https://doi.org/10.1111/j.1365-2486.2009.01935.x

923   Olsson, P.-O., Heliasz, M., Jin, H., Eklundh, L., 2017. Mapping the reduction in gross primary productivity

924   in subarctic birch forests due to insect outbreaks. Biogeosciences 14, 1703-1719. https://doi.org/10.5194/bg-

925   14-1703-2017

926   Parker, T.C., Subke, J.-A., Wookey, P.A., 2015. Rapid carbon turnover beneath shrub and tree vegetation is

927   associated with low soil carbon stocks at a subarctic treeline. Global Change Biology 21(5), 2070-2081.

928   https://doi.org/10.1111/gcb.12793

929   Parker, T.C., Sadowsky, J., Dunleavy, H., Subke, J.-A., Frey, S.D., Wookey, P.A., 2017. Slowed

930   biogeochemical cycling in Sub-arctic birch forest linked to reduced mycorrhizal growth and community

931   change after a defoliation Event. Ecosystems 20, 316-330. https://doi.org/10.1007/s10021-016-0026-7

932   Paterson, E., Sim, A., Davidson, J., Daniell, T.J., 2016. Arbuscular mycorrhizal hyphae promote priming of

933   native soil organic matter mineralisation. Plant and Soil 408, 243-254. https://doi.org/10.1007/s11104-016-

934   2928-8

935 Peršoh, D., Borken, W., 2017. Impact of woody debris of different tree species on the microbial activity and

936 community of an underlying organic horizon. Soil Biology and Biochemistry 115, 516-525.

937 https://doi.org/10.1016/j.soilbio.2017.09.017.

938 Philpott, T.J., Prescott, C.E., Chapman, W.K., Grayston, S.J., 2014. Nitrogen translocation and accumulation

939 by a cord-forming fungus (Hypholoma fasciculare) into simulated woody debris. Forest Ecology and

940 Management 315:121-128. https://doi.org/10.1016/j.foreco.2013.12.034

941 R Core Team, 2013. R: A language and environment for statistical computing. R Foundation for Statistical

942 Computing, Vienna, Austria. URL http://www.R-project.org/.

943 Rapalee, G., Trumbore, S. E., Davidson, E. A., Harden, J. W., Veldhuis, H., 1998. Soil carbon stocks and

944 their rates of accumulation and loss in a boreal forest landscape. Global Biogeochemical Cycles 12(4), 687-

945 701. https://doi.org/10.1029/98GB02336

946 Read, D.J., Perez-Moreno, J., 2003. Mycorrhizas and nutrient cycling in ecosystems – a journey towards

947 relevance? New Phytologist 157(3), 475-492. https://doi.org/10.1046/j.1469-8137.2003.00704.x

948 Rinne, K.T., Rajala, T., Peltoniemi, K., Chen, J., Smolander, A., Mäkipää, R., 2017. Accumulation rates and

949 sources of external nitrogen in decaying wood in a Norway spruce dominated forest. Functional Ecology 31,

950 530-541. https://doi.org/10.1111/1365-2435.12734

951 Rousk, K., Michelsen, A., 2017. Ecosystem nitrogen fixation throughout the snow-free period in subarctic

952 tundra: effects of willow and birch litter addition and warming. Global Change Biology 23(4), 1552-1563.

953 https://doi.org/10.1111/gcb.13418

954 Rundqvist, S., Hedenås, H., Sandström, A., Emanuelsson, U., Eriksson, H., Jonasson, C., Callaghan, T. V.,

955 2011. Tree and shrub expansion over the past 34 years at the tree-line near Abisko, Sweden. Ambio 40(6),

956 683-692. https://doi.org/10.1007/s13280-011-0174-0

957 Russell, M.B., Fraver, S., Aakala, T., Gove, J.H., Woodall, C.W., D'Amato, A.W., Ducey, M.J., 2015.

958 Quantifying carbon stores and decomposition in dead wood: A review. Forest Ecology and Management 350,

959 107-128. https://doi.org/10.1016/j.foreco.2015.04.033

960   Sandén, H., Mayer, M., Stark, S., Sandén, T., Nilsson, L.O., Jepsen, J. U., Wäli, P.R., Rewald, B., 2020. Moth

961   outbreaks   reduce   decomposition   in   Subarctic   forest   soils.   Ecosystems   23,   151-163.

962   https://doi.org/10.1007/s10021-019-00394-6

963   Saravesi, K., Aikio, S., Wäli, P.R., Ruotsalainen, A.L., Kaukonen, M., Huusko, K., Suokas, M., Brown, S.P.,

964   Jumpponen, A., Tuomi, J., Markkola, A., 2015. Moth outbreaks alter root-associated fungal communities in

965   Subarctic mountain birch forests. Microbial Ecology 69, 788-797. https://doi.org/10.1007/s00248-015-0577-

966   8

967   Schielzeth, H., Dingemanse, N.J., Nakagawa, S., Westneat, D.F., Allegue, H., Teplitsky, C., Réale, D.,

968   Dochtermann, N.A., Garamszegi, L.Z., Araya-Ajoy, Y.G., 2020. Robustness of linear mixed-effects models

969   to violations of distributional assumptions. Methods Ecol Evol. 2020; 11: 1141– 1152.

970   https://doi.org/10.1111/2041-210X.13434

971   Schmidt, M., Torn, M., Abiven, S., Dittmar, T., Guggenberger, G., Janssens, I.A., Kleber, M., Kögel-

972   Knabner, I., Lehmann, J., Manning, D.A.C., Nannipieri, P., Rasse, D.P., Weiner, S., Trumbore, S.E., 2011.

973   Persistence of soil organic matter as an ecosystem property. Nature 478, 49-56.

974   https://doi.org/10.1038/nature10386

975   Shahzad, T., Chenu, C., Genet, P., Barot, S., Perveen, N., Mougin, C., Fontaine, S., 2015. Contribution of

976   exudates, arbuscular mycorrhizal fungi and litter depositions to the rhizosphere priming effect induced by

977   grassland species. Soil Biology and Biochemistry 80, 146-155 https://doi.org/10.1016/j.soilbio.2014.09.023.

978   Silfver, T., Heiskanen, L., Aurela, M., Myller, K., Karhu, K., Meyer, N., Tuovinen, J.-P., Oksanen, E.,

979   Rousi, M., Mikola, J., 2020. Insect herbivory dampens Subarctic birch forest C sink response to warming.

980   Nature Communications 11, 2529. https://doi.org/10.1038/s41467-020-16404-4

981   Simard, S.W., Durall, D.M., 2004. Mycorrhizal networks: a review of their extent, function, and importance.

982   Canadian Journal of Botany 82, 1140-1165. https://doi.org/10.1139/b04-116

983   Sjögersten, S., Wookey, P.A., 2004. Decomposition of mountain birch leaf litter at the forest-tundra ecotone

984   in the Fennoscandian mountains in relation to climate and soil conditions. Plant and Soil 262, 215-227.

985   https://doi.org/10.1023/B:PLSO.0000037044.63113.fe

986 Smith, A., Granhus, A., Astrup, R., 2016. Functions for estimating belowground and whole tree biomass of

987 birch in Norway. Scandinavian Journal of Forest Research 31, 568-582,

988 https://doi.org/10.1080/02827581.2016.1141232

989 Stark, S., Ylänne, H., Kumpula, J., 2021. Recent mountain birch ecosystem change depends on the seasonal

990 timing of reindeer grazing. Journal of Applied Ecology 58, 941–952. https://doi.org/10.1111/1365-

991 2664.13847

992 Starr, M., Hartman, M., Kinnunen, T., 1998. Biomass functions for mountain birch in the Vuoskojärvi

993 Integrate Monitoring area. Boreal Environment Research 3, 297-303.

994 Štursová, M., Šnajdr, J., Cajthaml, T., Bárta, J., Šantrůčková, H., Baldrian, P., 2014. When the forest dies:

995 the response of forest soil fungi to a bark beetle-induced tree dieback. The ISME Journal 8, 1920-1931.

996 https://doi.org/10.1038/ismej.2014.37

997 Sun, L., Ataka, M., Kominami, Y., Yoshimura, K., 2017. Relationship between fine-root exudation and

998 respiration of two Quercus species in a Japanese temperate forest. Tree Physiology 37(8), 1011-1020.

999 https://doi.org/10.1093/treephys/tpx026

1000 Tenow, O. 1996. Hazards to a mountain birch forest - Abisko in perspective. Ecological Bulletins 45, 104-

1001 114. https://www.jstor.org/stable/20113188

1002 Tømmervik, H., Johansen, B., Tombre, I., Thannheiser, D., Høgda, K.A., Gaare, E., Wielgolaski, F.E., 2004.

1003 Vegetation changes in the nordic mountain birch forest: the influence of grazing and climate change. Arctic,

1004 Antarctic, and Alpine Research 36(3), 323-332. 10.1657/1523-0430(2004)036[0323:VCITNM]2.0.CO;2

1005 Tybirk, K., Nilsson, M.-C., Michelsen, A., Kristensen, H.L., Shevtsova, A., Strandberg, M.T., Johansson, M.,

1006 Nielsen, K.E., Riis-Nielsen, T., Strandberg, B., Johnsen, I., 2000. Nordic Empetrum dominated ecosystems:

1007 Function and susceptibility to environmental changes. Ambio, 29, 90-97. http://dx.doi.org/10.1579/0044-

1008 7447-29.2.90

1009 Vuojala-Magga, T., Turunen, M.T., 2015. Sámi reindeer herders' perspective on herbivory of subarctic

1010 mountain birch forests by geometrid moths and reindeer: a case study from northernmost Finland.

1011 *SpringerPlus* 4, 134. https://doi.org/10.1186/s40064-015-0921-y

1012 Wang, H., Xu, W., Hu, G., Dai, W., Jiang, P., Bai, E., 2015. The priming effect of soluble carbon inputs in

1013 organic and mineral soils from a temperate forest. Oecologia 178, 1239-1250.
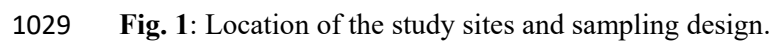
1014 https://doi.org/10.1007/s00442-015-3290-x

1015 Wilmking, M., Harden, J., Tape, K., 2006. Effect of tree line advance on carbon storage in NW Alaska.

1016 Journal of Geophysical Research Biogeosciences 111(G2). https://doi.org/10.1029/2005JG000074

1017 WRB, IUSS Working Group. 2015. World Reference Base for Soil Resources 2014, update 2015

1018 International soil classification system for naming soils and creating legends for soil maps. World Soil

1019 Resources Reports No. 106. FAO. Rome.

1020 Ylänne, H., Madsen, R.L., Castaño, C., Metcalfe, D.B., Clemmensen, K.E., 2021. Reindeer control over

1021 subarctic treeline alters soil fungal communities with potential consequences for soil carbon storage. Global

1022 Change Biology 27, 4254-4268. https://doi.org/10.1111/gcb.15722.

1023 Zackrisson, O., DeLuca, T.H., Gentili, F., Sellstedt, A., Jäderlund, A., 2009. Nitrogen fixation in mixed

1024 Hylocomium splendens moss communities. Oecologia 160, 309-319. https://doi.org/10.1007/s00442-009-

1025 1299-8

1026

1028

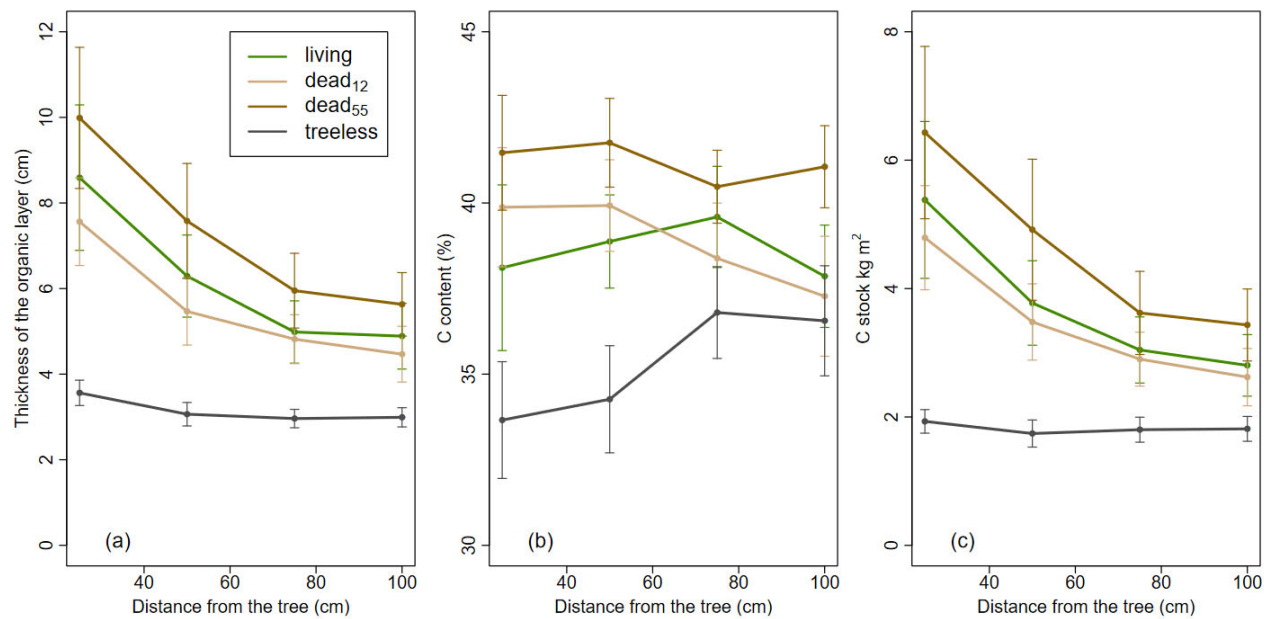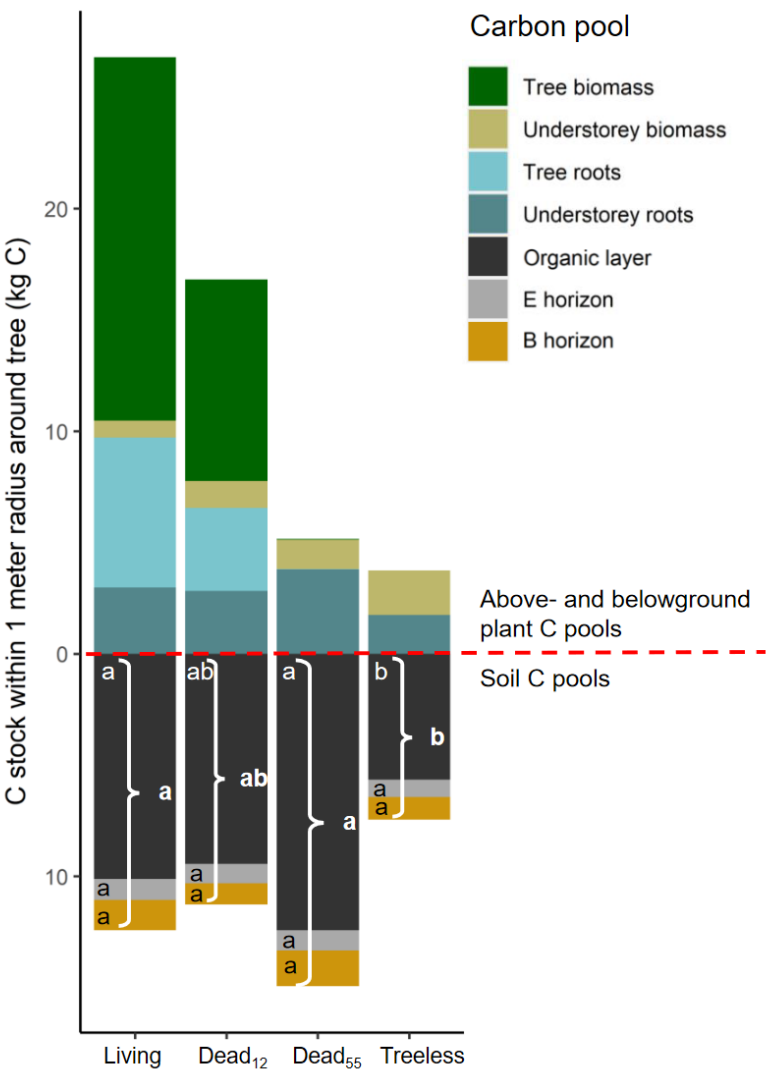**Fig. 1**: Location of the study sites and sampling design.

1030

Fig. 2: Pictures of tree status: a) living tree, b) dead$_{12}$ tree, c) dead$_{55}$ tree, d) treeless tundra. Living and dead
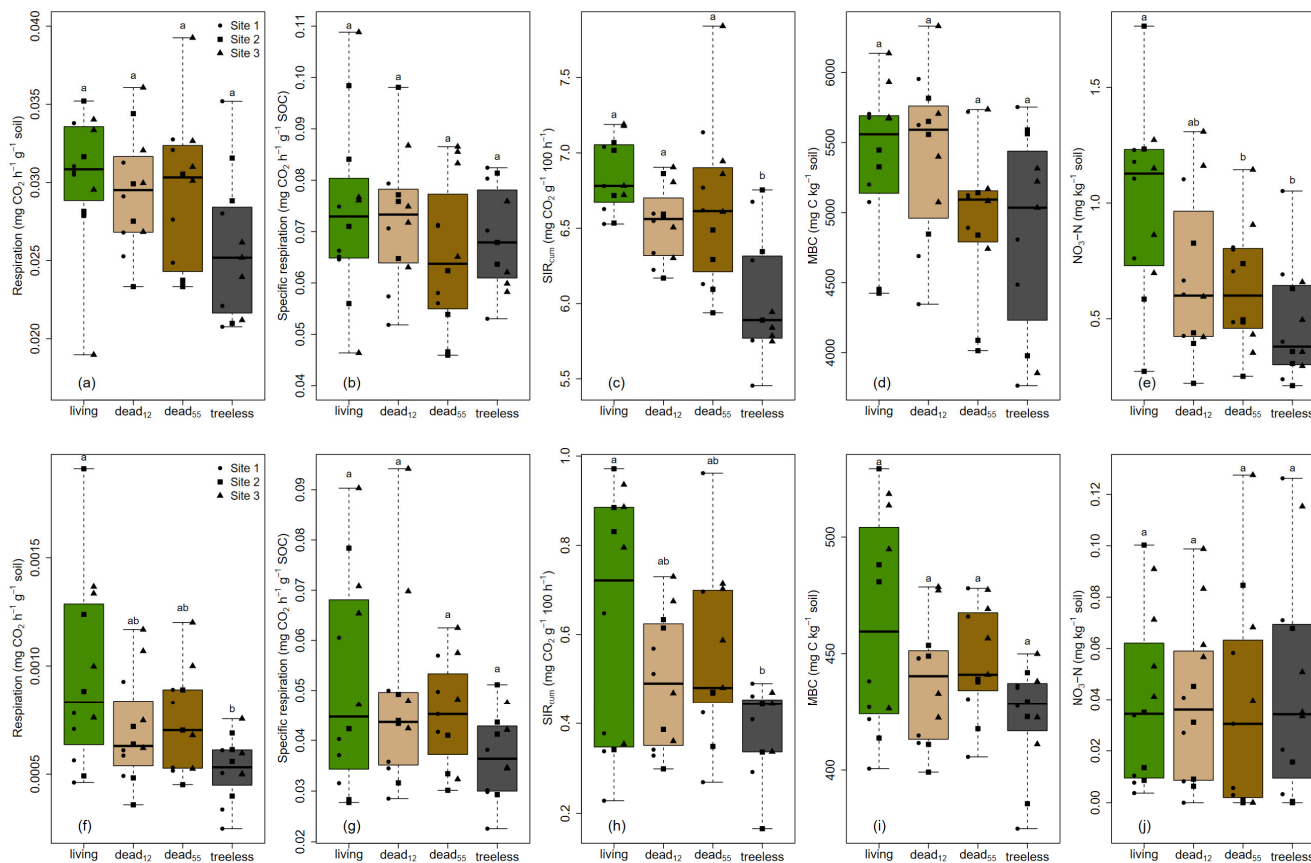
trees are scattered sparsely in the landscape.

1033

Fig. 3: Thickness (a), C contents (b), and C stocks (c) of the organic layer. Mean and standard error are
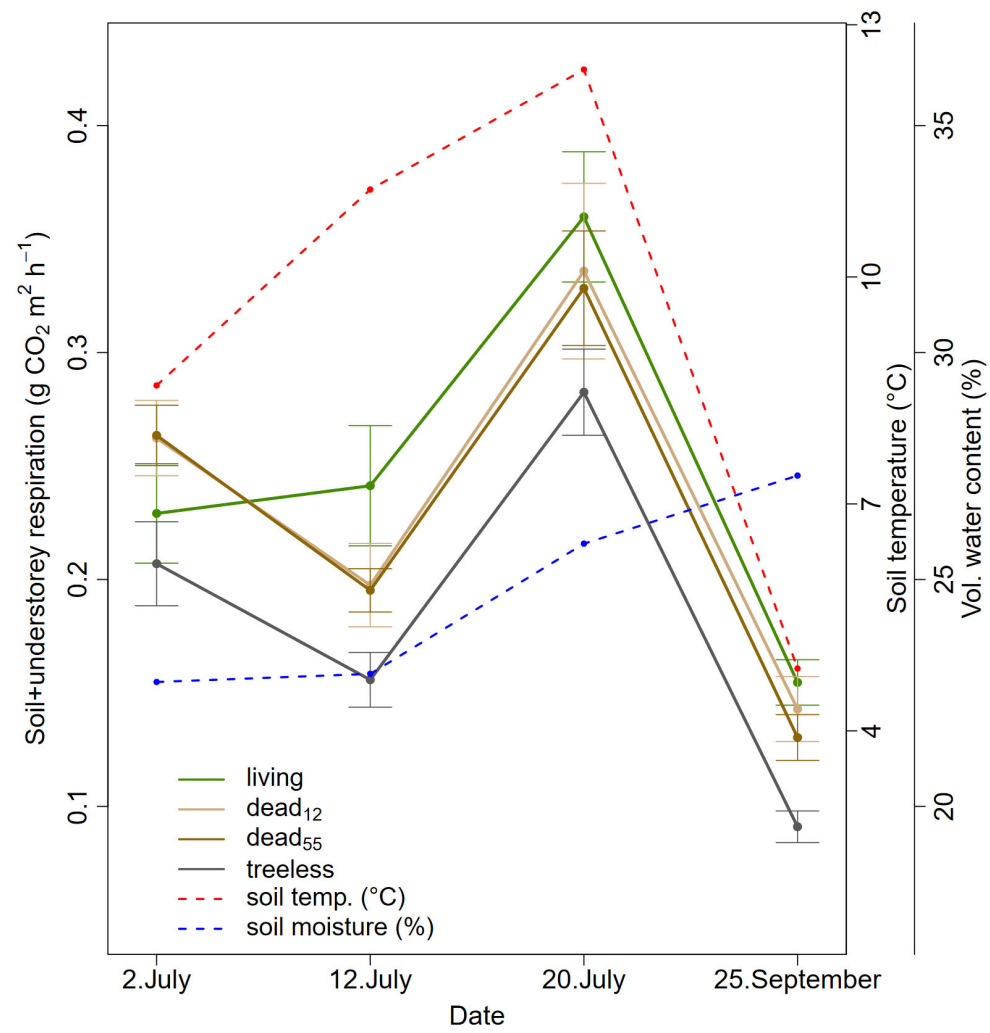
presented.

1036

1037

Fig. 4: Total C stocks averaged over the three sites for the investigated area of 1 m radius around a tree or plot center of the treeless tundra (3.14 m²). Soil was sampled up to the bedrock, i.e. total SOC stocks were measured. Letters indicate significance differences of soil C pools.
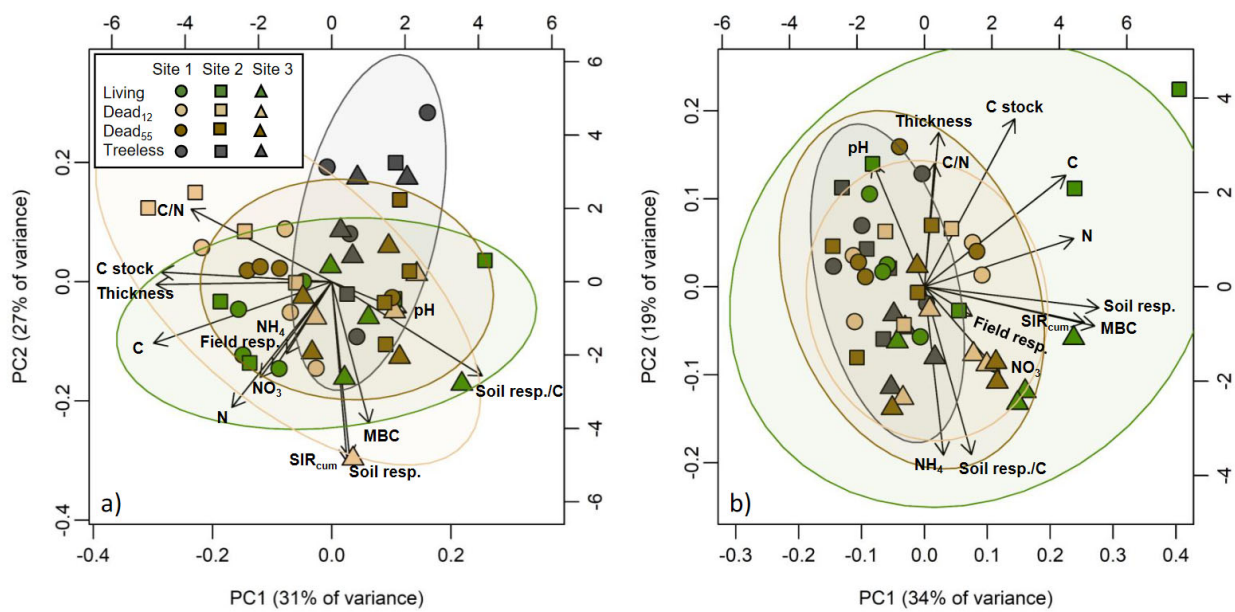
1041

Fig. 5: Effect of tree status on soil properties in the organic layer (upper row) and mineral soil (lower row). Whiskers show the minimum and maximum value, respectively. a) Soil respiration (organic layer), b) SOC-specific respiration (organic layer), c) cumulative CO_2 evolution within 100h after glucose addition (organic layer), d) microbial biomass (organic layer), e) NO_3-N (organic layer), f) soil respiration (mineral soil), g) SOC-specific respiration (mineral soil), h) cumulative CO_2 evolution within 100h after glucose addition (mineral soil), i) microbial biomass (organic layer), e) NO_3-N (mineral soil). In each figure, different letters indicate significant differences ($p<0.05$). Different symbols indicate the distribution at the three sites.

1047

1048   **Fig. 6**: Soil + understorey respiration, soil temperature, and volumetric soil water content. Mean and standard error are presented.

1049

Fig. 7: Principal component analysis of a) organic layer, and b) mineral soil. Principal component scores of samples are represented by symbols, and loadings of variables are represented by vectors. Increasing vector distance from the plot center reflects a stronger influence on the respective principal component. The angle between vectors indicates the correlation between variables: a small angle indicates a positive correlation, a 90°C vector indicates no correlation, and diverging vectors (i.e. 180°C) indicate negative correlations. Ellipses show the 90% confidence interval for the respective tree status. Thickness refers to the thickness of the organic layer or mineral soil, respectively; C and N refer to concentrations (%); C stock is the calculated SOC stock at 50 cm distance; Soil resp./C is the SOC-specific respiration rate; SIR_{cum} is the cumulative CO_2 evolution within 100h after glucose addition; Soil resp. is the soil respiration rate under lab conditions; Field resp. is soil+understorey respiration measured in the field; and MBC is microbial biomass carbon.